teasome. Each of the three β subunits preferentially cleaves an acidic, basic, or hydrophobic residue, activities often referred to as caspase-like, trypsin-like, or chymotrypsin-like, respectively.

In vertebrates, there are three additional IFN-γ–induced subunits: β1i, β2i, and β5i. These are preferentially incorporated into the 20S proteasome in place of the standard subunits to form the immunoproteasome in immune cells such as macrophages, T and B cells, and dendritic cells, whereas their expression is low in nonlymphoid peripheral tissues. This results in more efficient production of MHC class I epitopes (12). The present study analyzed the activity of proteasomes with a mutated β5i subunit, and the subsequent inflammatory signal transduction pathways in mutant cells. The results suggest that the *PSMB8* mutation evokes an inflammatory response in humans, and that the p38 pathway may play an important role in inflammation in NNS patients.

Recently, a different mutation in the *PSMB8* gene was reported in patients with a disease similar to, but distinct from, NNS: an autosomal recessive syndrome of joint contracture, muscular atrophy, microcytic anemia, and panniculitis-associated lipodystrophy (JMP) (13, 14). The mutation in JMP syndrome, T75M, causes a reduction in chymotrypsin-like activity only, without disrupting the activity of other peptidases (13). In contrast, the G201V mutation identified in NNS patients results in the loss of all peptidase activity because of assembly defects and reduced proteasome levels. Thus, the discovery of *PSMB8* mutations in these related diseases indicates the presence of a distinct class of proteasome-associated autoinflammatory disorders.

Results

Clinical Features of NNS Patients. National surveillance in Japan confirms that only around 10 NNS patients are alive today. Therefore, preserved fibroblasts from an autopsy case (patient 1) were provided for genetic analysis, following approval by the local ethical committee. Of the living cases, written informed consent to undertake genetic and molecular analyses was obtained from six patients. The clinical features of all seven cases are summarized in Table S1. Patients 1, 2, and 4 were born to consanguineous parents and their clinical features have been described previously (Fig. S1*A*) (6, 8). The other patients are sporadic cases collected for this study and were born in the limited area between south Osaka and Wakayama. A diagnosis of NNS is not difficult owing to the characteristic features, including the thin facial appearance and long clubbed fingers (Fig. S1*B*). The clinical course throughout childhood was variable: from no medical consultation in the case of patient 7, to administration of oral steroids since infancy in patients 3 and 6. Partial lipomuscular atrophy with long clubbed fingers plus a pernio-like, heliotrope-like, or nodular erythema-like skin rash were observed in all cases, and periodic fever and joint contractures in most but not all. Wheras hyperhidrosis was also observed in some cases, short stature and low IQ were seen only in patients 6 and 1, respectively. Indeed, patient 6 was treated with growth hormone, although growth retardation in this case may have been due, in part, to oral steroids. Chronic inflammation, indicated by elevated ESR and hyper-γ-globulinemia, were observed in all patients, and microcytic anemia, high serum creatine phosphokinase (CPK), hepatosplenomegaly, and basal ganglia calcification were present in most, but not all. Notably, various autoantibodies (with a mildly elevated titer of antinuclear antibodies) were detected in half of the patients. The most striking differences between NNS and JMP are the absence of fever in JMP syndrome and the absence of seizures in NNS (14) (Table S1).

Genetic Mapping and Mutation Searches. We examined genomic DNA samples from five patients (patients 1–5) and three unaffected siblings of patient 4 using an Affymetrix GeneChip Human Mapping 500K array set (Nsp I and Sty I arrays), and the BRLMM genotyping algorithm. Because the runs of homozygosity (ROHs) shared by all patients were expected to be candidate regions containing the gene responsible for the disease, we identified a region spanning 1.1 Mb on chromosome 6p21.31–32 [from 32,798,004–33,903,106; National Center for Biotechnology Information (NCBI) build 36.1] as the sole candidate region responsible for NNS (Fig. 1*A*). We directly sequenced 436 coding exons in the 44 genes within this candidate region, including the splicing sites. A single nonsynonymous variation (not registered in the dbSNP database) was identified in exon 5 of *PSMB8* (NM_148919 in the NCBI database), designated *LMP7* or *RING10*, which encodes the LMP7 protein (β5i subunit) of the immunoproteasome. This mutation was a guanine to thymine transversion at nucleotide position 602 (c.602G > T) (Fig. 1*B*). Haplotype analysis indicated that the G201V mutation was probably introduced into the Japanese population by a single founder, as the haplotype around this mutation was identified in all patients (Fig. S1*C*). Gly201, which is a highly conserved residue in the β5i subunit (Fig. 1*C*) and among mature proteasome subunits in vertebrates (Fig. S1*D*), is substituted by Val (G201V) (Fig. 1*B*).

Impaired Immunoproteasome Assembly and Peptidase Activity. In silico modeling of the mutant β5i ($\beta5i^{G201V}$) subunit was used to infer the conformational impact of this mutation because the assembly of the proteasome is a highly orchestrated and complex process (9, 15). The β5i subunit is cleaved between amino acid residues Gly72 and Thr73 to yield the active form (16), in which the catalytic center is generated by Thr73, Asp89, Arg91, and Lys105. The mutated residue at position 201 was located at the edge of the S8 β-sheet of β5i and was close to its catalytic threonine residue Thr73 (Fig. 2*A*). The G201V substitution caused conformational changes not only in Thr73 but also in Lys105 within the catalytic center (Fig. S2). The mutation resulted in further conformational changes in the S8–H3 loop located at the

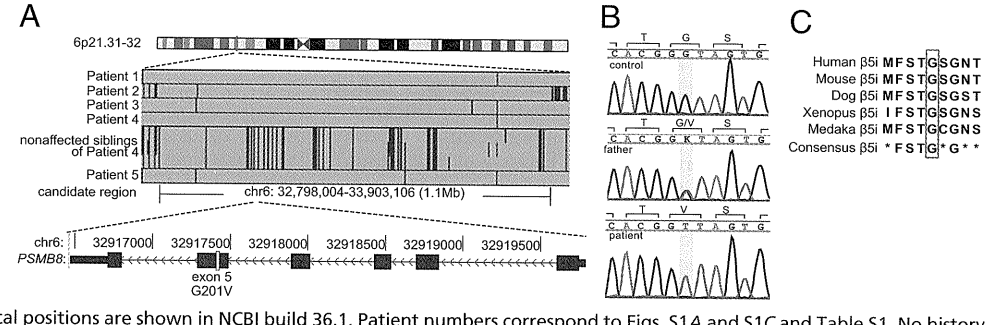

Fig. 1. SNP microarray-based homozygosity mapping and mutation search. (*A*) Homozygosity mapping for NNS patients and nonaffected siblings. ROH regions were detected using a hidden Markov model-based algorithm. The sole candidate region identified within 6p21.31–32 is shown. Green vertical lines indicate heterozygous SNPs and the background gray area indicates a region without heterozygous SNP calls. To be conservative, we did not regard isolated single heterozygous calls as delimiting ROH regions. The physical positions are shown in NCBI build 36.1. Patient numbers correspond to Figs. S1*A* and S1*C* and Table S1. No history of consanguineous marriage was apparent for patients 3 and 5, according to the family history interview. (*B*) Chromatograms for a control, a patient's father, and a patient. A mutation in *PSMB8* exon 5 identified in NNS patients by sequencing is highlighted in yellow. (*C*) Amino acid comparisons with other species. The glycine at the mutation site (red box) is highly conserved among vertebrates.

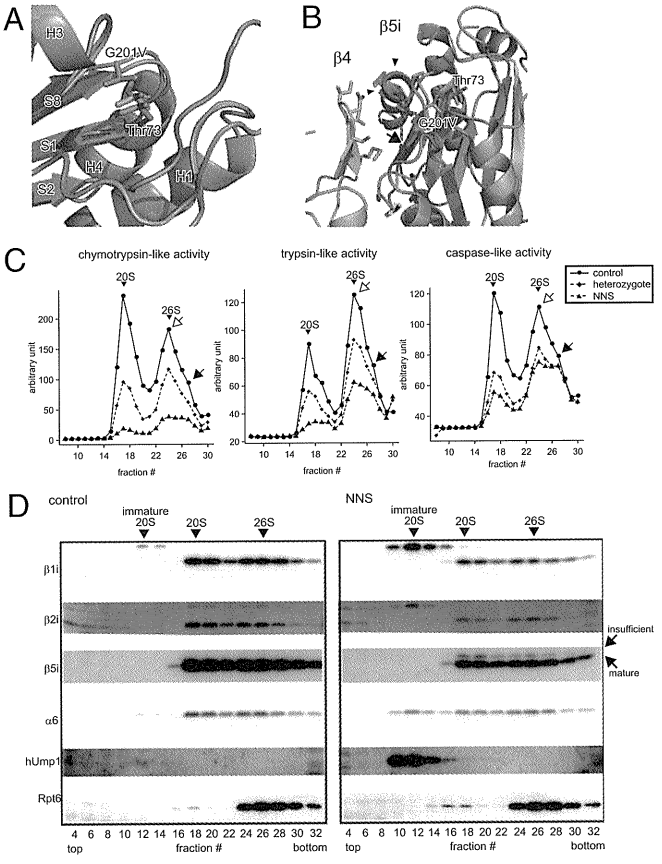

Fig. 2. G201V mutation in β5i reduces proteasome activity in immunoproteasome-expressing cells. (*A*) Close-up view of the mutation site (G201V) within β5i. Structural models of G201V β5i (orange) and wild-type β5i (green) were created from the β5-subunit structure [Protein Data Bank (PDB) ID code 1IRU]. The secondary structure elements for β5i are labeled. Val201 and Thr73 are shown in the stick model. Thr73 is a catalytic residue of β5i. (*B*) A ribbon diagram of the β4–β5i complex. The arrow shows the difference in the β-sheet between β5i (green) and β5i^{G201V} (orange). Arrowheads show the protruding S8–H3 loop of β5i^{G201V}. (*C*) Peptidase activity of LCLs. Extracts were fractionated by glycerol gradient centrifugation (8–32% glycerol from fraction 1–32). Arrowheads indicate the peak positions of the 20S and 26S proteasomes (open arrows, single-capped 26S; closed arrows, double-capped 26S). (*D*) Western blot analysis of fractionated total LCL extracts. Western blot analysis of proteasome subunits from fractions 1–32 fractionated in *C*. The sedimenting positions of the immature 20S, 20S, and 26S proteasomes are indicated by arrowheads. The mature and incompletely cleaved β5i^{G201V} subunits are indicated by arrows. The mature β5i subunit is cleaved within a C-terminal polypeptide between Gly72 and Thr73. The insufficiently cleaved β5i subunit is probably cleaved at a site toward the N terminus site, yielding a fragment with a higher molecular weight. The same amount of protein was subjected to glycerol gradient ultracentrifugation. The level of proteasome is reduced in NNS patients. Control, LCL extract from healthy control; NNS, LCL extract from patient with NNS.

interface between β4 and β5i, which affected the surface contact of β5i with the adjacent β4 subunit (Fig. 2*B*). These results suggest that the G201V mutation affects both β5i catalytic activity and assembly of the 20S proteasome.

According to Sijts and Kloetzel (17), the β1 subunit has a caspase-like function, the β2 subunit has trypsin-like activity, and the β5 subunit has chymotrypsin-like activity. Although it has not been clearly confirmed which of the immunoproteasome subunits possess which peptidase activity, it is generally thought that β5i has chymotrypsin-like activity. We next examined the influence of the β5i mutation on proteasome peptidase activity. Extracts from immortalized lymphoblastoid cell lines (LCLs) that constitutively expressed the immunoproteasome, rather than the standard proteasome, were obtained from an NNS patient, his heterozygous parent, and a healthy control, and were separated by glycerol gradient centrifugation. The fractions were then assayed for chymotrypsin-like, trypsin-like, and caspase-like activity mediated by the 20S/26S proteasomes. The results showed that not only was chymotrypsin-like activity markedly decreased in NNS cells, but the other two enzyme-like activities were also decreased (Fig. 2*C*).

Reduced Proteasome Levels. To gain further insight into the molecular mechanisms affecting peptidase activity in the mutant cells, the glycerol density gradient fractions were subjected to Western blot analysis (Fig. 2*D*). Assembly of the mammalian 20S proteasome begins with the formation of the α-ring in conjunction with a dedicated assembly chaperone, PAC1-4. The β-ring is then formed on the α-ring with the aid of another chaperone, hUmp1, resulting in the formation of half-sized immature proteasomes. The immature proteasomes then dimerize to form the 20S proteasome accompanied by cleavage of β-subunit propeptides and the degradation of hUmp1 (9). Our most noteworthy finding was the accumulation of immature 20S proteasome precursors in NNS cells before incorporation of β5i and dimerization, as indicated by the presence of the proforms of β1i and β2i, α6 and hUmp1, and the absence of β5i (Fig. 2*D*, fractions 10–14) (18). Computer modeling suggests that this assembly defect could be due to the fact that β5i, β4, and β6 line up next to each other and that the interaction between mutant β5i^{G201V} and β4 may be disturbed (Fig. 2*B*). The reduction in peptidase activity was unlikely due to differences in the ability of 20S to associate with 19S RP, because single-capped and double-capped 26S proteasomes were detected in the glycerol fractions from an NNS patient and control LCLs (Fig. 2*C*). The assembly defect caused a reduction in the number of 20S and 26S proteasomes in NNS cells (Fig. 2*D*), which accounts for the observed decrease in activity of all three peptidases. Another intriguing observation was that a portion of the β5i^{G201V} subunit incorporated into the mature proteasome appeared as a slower migrating band, suggesting the presence of an insufficiently cleaved form of β5i^{G201V} (Fig. 2*D*) (16). This may have contributed to the markedly reduced chymotrypsin-like activity seen in NNS cells compared with the other two peptidase activities.

Decreased Proteolytic Activity and Accumulation of Ubiquitinated and Oxidized Proteins. To examine proteolytic activity in vitro, the ornithine decarboxylase (ODC) degradation assay was performed (19). Proteolytic activity was significantly decreased in mutant proteasomes (Fig. 3*A*). As a consequence of the altered proteasome levels and incomplete cleavage of the subunits, proteolytic activity decreased and ubiquitinated proteins accumulated in LCLs (Fig. 3*B*) and fibroblasts from NNS patients (Fig. 3*C*). In particular, there was an obvious accumulation of K48 polyubiquitinated proteins in fibroblasts (Fig. 3*C*).

Because the immunoproteasome is important for degrading oxidized proteins and defective ribosomal products (20), we examined whether such proteins accumulated in NNS cells. We found that the level of oxidized proteins increased in cultured NNS fibroblasts and after stimulation with IFN-γ (Fig. 3*D*). Taken together, these results show that the G201V substitution within β5i severely impairs assembly of the immunoproteasome, leading to decreased proteasome levels and activity in β5i-expressing cells.

We then examined whether the defect in proteasome activity was apparent in situ in NNS patients. We stained skin biopsy sections obtained from an NNS patient and used sections from a monocytic fasciitis patient as a control. CD68 is a marker for monocyte/macrophages, a cell type known to predominantly express the immunoproteasome rather than the standard proteasome (21). Inflammatory responses characterized by the infiltration of numerous CD68$^+$ cells into the skin were observed in both NNS and fasciitis samples. However, the CD68$^+$ cells in the NNS sec-

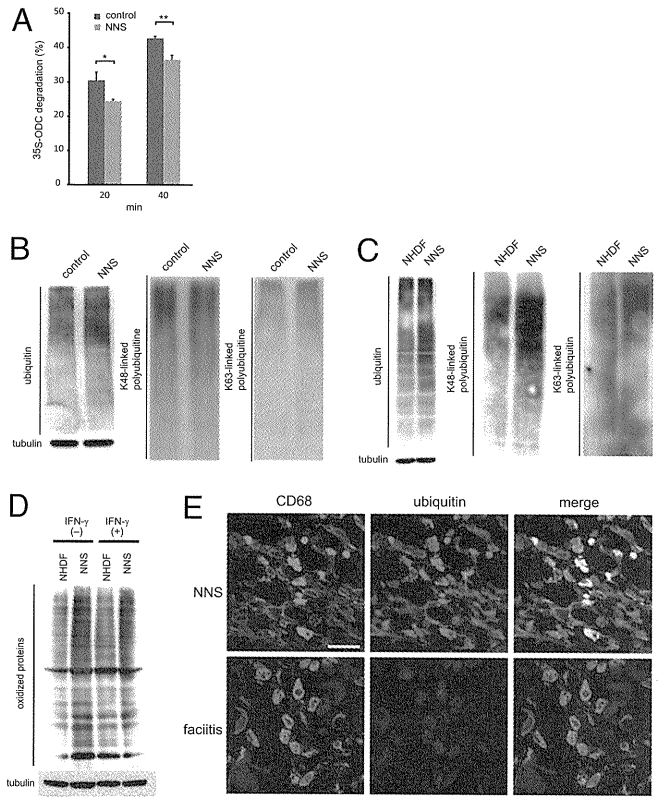

Fig. 3. Decrease of proteolytic activity and accumulation of poly-ubiquitinated and oxidized proteins in NNS cells. (*A*) In vitro proteolytic activity of the mutant proteasome. Degradation of recombinant ^{35}S-labeled ODC was expressed as % total ODC as described previously (11). Error bars indicated the SD of the mean ($n = 3$). $*P < 0.05$, $**P < 0.01$. (*B* and *C*) Accumulation of ubiquitinated proteins in LCLs (*B*) and fibroblasts (*C*). Western blot analysis of ubiquitinated proteins using an antiubiquitin antibody (*Left*), an anti-K48 polyubiquitinated protein antibody (*Middle*), and an anti-K63 polyubiquitinated protein antibody (*Right*). Tubulin was used as a loading control (*Lower*). NHDF, adult normal human dermal fibroblasts. (*D*) Levels of oxidized proteins determined by Oxyblot. NHDF and NNS fibroblasts were stimulated with or without 100 units of IFN-γ for 24 h. Tubulin was used as a loading control. (*E*) Immunofluorescence staining of CD68 and ubiquitinated proteins. Staining for CD68 (green) and ubiquitinated proteins (red) in skin sections from an NNS patient and a fasciitis patient. NNS ubiquitin signals showed a 4.7-fold increase with ImageJ (http://rsb.info.nih.gov/ij/) compared with fasciitis signals. (Scale bar, 10 μm.)

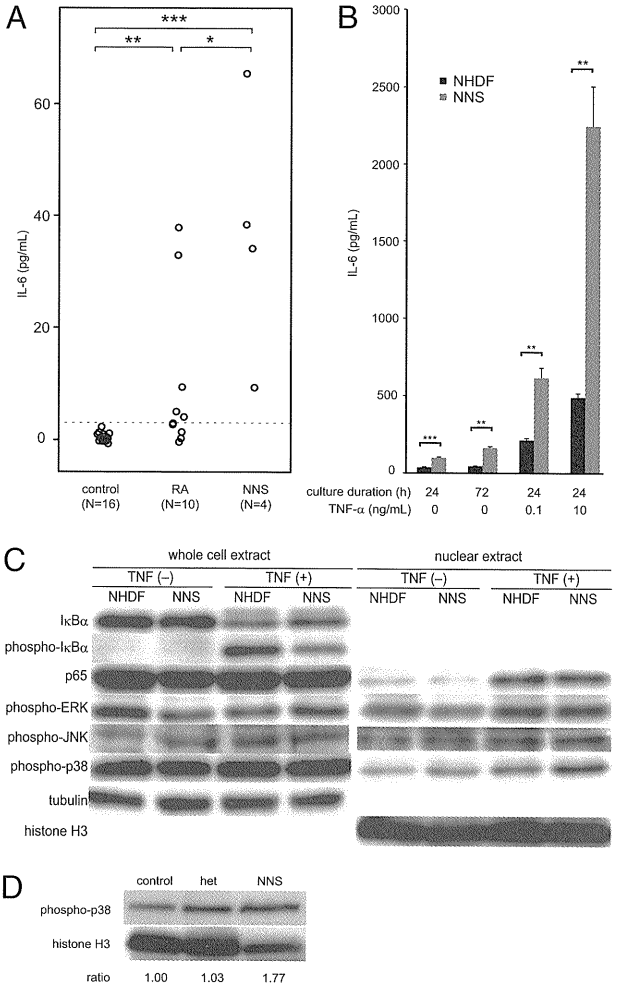

Fig. 4. Analyses of the level of IL-6 in NNS and the signal transduction system related to cytokine production. (*A*) IL-6 concentrations in sera from healthy controls, patients with NNS, and patients with rheumatoid arthritis. IL-6 levels in sera were determined by ELISA. (*B*) IL-6 production by cultured fibroblasts. The concentrations of IL-6 in conditioned media were determined by ELISA (in triplicate). (*C*) Western blot analysis for NF-κB and MAPK. Whole cell extracts and nuclear extracts were immunoblotted using antibodies against IκBα, p-IκBα, p65, p-ERK, p-JNK, and p-p38. (*D*) Western blot analysis of p-p38 in peripheral blood lymphocytes. Nuclear extracts from the peripheral blood lymphocytes of a healthy control, a heterozygous family member, and a NNS patient were blotted and visualized with anti–p-p38. Error bars indicate SD of the mean. $*P < 0.05$, $**P < 0.01$, $***P < 0.001$ [Mann-Whitney *u* test (*A*) and two-tailed Welch's *t* test (*B*)]. Signal intensities were quantified using ImageJ and expressed as fold changes relative to a healthy control normalized to histone H3 (*D*).

tions were strongly positive for ubiquitin, whereas ubiquitin was only faintly detectable in the fasciitis sections (Fig. 3*E*).

Increased IL-6 and IP-10 Levels in NNS Patient Sera and Signal Transduction in NNS Fibroblasts. We next screened NNS patient sera for inflammatory cytokines using a multiplex bead-based ELISA on a suspension array. The results showed a significant increase in the levels of interleukin (IL)-6, IFN-γ–inducible protein (IP)-10, granulocyte colony stimulating factor, and monocyte chemoattractant protein-1 (Fig. S3*A*). IL-6 was of particular interest because it is a pleiotropic cytokine with a wide range of biological activities, and it plays a key role of immune regulation, hematopoiesis, oncogenesis, and inflammation (22–24). Increased IL-6 levels in NNS sera were confirmed using a standard ELISA (Fig. 4*A*). IL-6 production was significantly higher in NNS patient fibroblasts than in healthy control fibroblasts both in the presence and absence of TNF-α (Fig. 4*B*). The serum concentration of IP-10 was also higher than that in healthy controls (Fig. S3 *A* and *B*). We measured the level of IP-10 in conditional media from cultured fibroblasts using an ELISA, but found no significant difference under the conventional culture condition, although NNS cells tended to overproduce IP-10 after stimulation with 10 ng/mL TNF-α (Fig. S3*C*).

We next investigated the various signal transduction pathways that could be responsible for IL-6 overproduction by NNS fibroblasts. Nuclear factor (NF)-κB and AP-1 are the two major transcription factors that induce proinflammatory cytokines, including IL-6 (25, 26). We used an EMSA to detect activated NF-κB in cells treated with TNF-α; however, no differences in the amount of the p65/p50 heterodimer were observed in nuclear extracts from NNS fibroblasts and healthy control fibroblasts (Fig. S4 *A* and *B*). Consistent with this result, IκBα degradation and nuclear translocation of NF-κB were not enhanced in NNS fibroblasts (Fig. 4*C*). Although activation of NF-κB is largely dependent on the ubiquitin–proteasome system, these results

suggest that decreased proteasome activity does not have much influence on the regulation of NF-κB signaling in NNS cells.

We next measured the molecules that activate AP-1, including JNK1/2/3, ERK1/2, and p38, by Western blot analysis (27, 28). The amount of phosphorylated p38 (p-p38) in the nuclear extracts from NNS fibroblasts was increased (Fig. 4*C*), irrespective of TNF-α stimulation; however, there was no obvious difference in the levels of JNK1/2/3 and ERK1/2 (Fig. 4*C*). We also observed increased levels of p-p38 in the nuclear extracts from NNS peripheral blood lymphocytes (Fig. 4*D*). The build-up of oxidized proteins and/or reactive oxygen species (ROS) within NNS fibroblasts may be one of the mechanisms responsible for the accumulation of p-p38 (29, 30).

Discussion

We have identified a point mutation in the gene encoding the immunoproteasome subunit β5i as the cause of NNS. This mutation interferes with the assembly of the 20S proteasome in cells expressing immunoproteasomes. The mutation is described as c.602G > T, and results in a Gly201 to Val (G201V) (NM_148919) substitution in the immunoproteasome β5i subunit. Although a heterozygous carrier showed reduced proteasome peptidase activity, carriers had no clinical symptoms. Thus, the NNS phenotype may be due to a reduction in total proteasome enzymatic activity below the threshold necessary for maintaining cellular homeostasis in homozygous individuals.

The *PSMB8* mutation, c.224C > T (Thr75Met), occurs in patients with JMP syndrome (13). Mutant β5i in JMP patients results in a clear reduction in chymotrypsin-like activity only, with no disruption of other peptidase activities. However, the G201V mutation we identified in NNS patients causes losses of all peptidase activity owing to assembly defects and reduced proteasome levels. The T75M mutation is probably rapidly incorporated to the proteasome complex during biogenesis and is specific for chymotrypsin-like activity. The differences between the JMP syndrome and NNS phenotypes, including cytokine production by various cells during inflammatory or noninflammatory states, need to be clarified because these differences could result from a reduction in chymotrypsin-like activity in JMP syndrome or from reductions in chymotrypsin-, trypsin-, and caspase-like activity in NNS. One of the main differences between NNS and JMP syndrome is the level of IFN-γ. IFN-γ levels are increased in JMP patients, but are within the normal range in NNS patients (Fig. S3*A*). The basis for this difference is unclear. It is possible that IFN-γ levels may not increase when all three peptidase activities are inhibited.

We also found increased IP-10 levels in patient sera using ELISA on suspension arrays. There were no significant differences in IP-10 levels between nonstimulated NNS fibroblasts and control cells, although NNS fibroblasts tended to overproduce IP-10 after stimulation with TNF-α (Fig. S3 *B* and *C*). This may reflect the proinflammatory state in NNS cells, or an increased sensitivity to cytokines (31). Because IP-10 is categorized as an inflammatory chemokine produced by various types of cells, it may play an important role in leukocyte homing to inflamed tissues and in perpetuating inflammation in various autoimmune diseases such as rheumatoid arthritis, systemic lupus erythematosus, systemic sclerosis, and multiple sclerosis (32). Thus, IP-10 may enhance inflammation in NNS patients and be associated with the autoantibody production that is occasionally observed.

A single base deletion in the 5′-UTR of hUmp1 causes keratosis linearis with ichthyosis congenita and sclerosing keratoderma (KLICK) syndrome, which is characterized by palmoplantar keratoderma (33) related to proteasome activity. This mutation results in changes in hUmp1 levels and alterations in the epidermal distribution of hUmp1 and proteasomal subunits. It is unclear how the proteasome functions in KLICK syndrome, although it is clear that disturbances in proteasome function cause clinical phenotypes in humans.

Studies in animal models indicate that cells deficient in various immunoproteasome subunits show poor CD8 responses when challenged with epitopes (34, 35) and may display alterations in the T-cell receptor (TCR) repertoire (36). In particular, β5i-deficient mice show increased susceptibility to pathogens, most likely due to the reduced efficiency of antigen presentation by β5i-deficient cells (12). Actually, in NNS patients, unresponsiveness to an intradermally applied purified protein derivative of *Mycobacterium tuberculosis* has been reported; however, there are no documented changes in susceptibility to pathogens, and no abnormalities in the number of any particular T-cell subset have been observed, apart from reduced NK activity (4). Conversely, there are no reports that β5i-deficient mice show the type of systemic inflammation observed in NNS patients.

In general, gene-deficient mice are very useful tools for analyzing the functions of target genes; however, the $\beta5i^{G201V}$ mutation shows a type of "enzymatic dominant-negative interference," which abrogates not only chymotrypsin-like activity (due to the mutation) but also the activity of the entire proteasome (due to defective assembly). Thus, it is not surprising that the phenotype seen in NNS is different from that seen in *Psmb8* knockout mice (12, 20) or after treatment with PR-957 inhibitors (37). Thus, analysis of patients with NNS and JMP syndrome and mice knocked in with these mutations would provide new insights into the function of the immunoproteasome in vivo.

Finally, we observed increased levels of p-p38 in nuclear extracts from NNS peripheral blood lymphocytes (Fig. 4*D*), although it remains unknown precisely how attenuation of proteasome activity causes accumulation of p-p38 in the nucleus. The

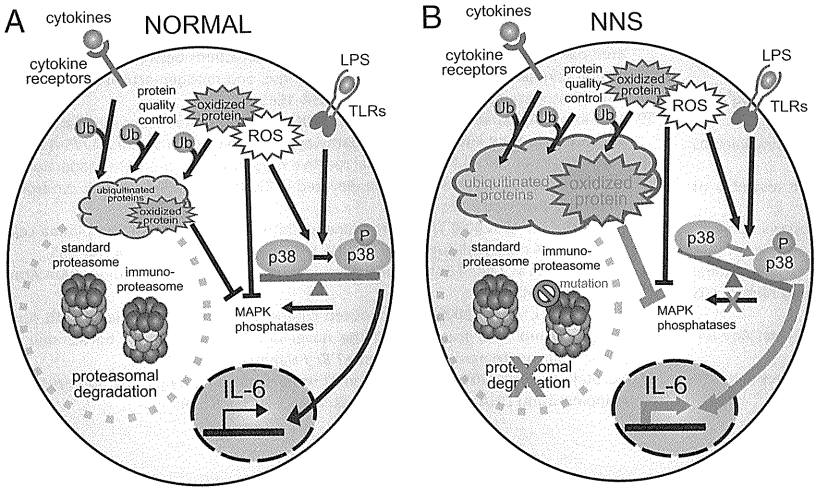

Fig. 5. Schematic model showing induction of inflammation in NNS patients with the *PSMB8* mutation. Our data are based on the scheme proposed by Bulua et al. (40). (*A*) In a normal cell, ubiquitinated or oxidized proteins generated by various stressors, including cytokines, are cleared by proteasomes. (*B*) The ubiquitinated and oxidized proteins accumulate in a cell with the *PSMB8* mutation (NNS cell). ROS and/or oxidized proteins may cause phosphorylation of p-38 to predominate over the nonphosphorylated form by inhibiting MAPK phosphatase or by activating MAPK.

accumulation of oxidized proteins and/or ROS in NNS fibroblasts may be one of the mechanisms responsible for the accumulation of p-p38 (29, 30, 38, 39). Increased p-p38 levels are in agreement with the proposed mechanism for TNFR1-associated periodic syndrome (TRAPS), which is another autoinflammatory syndrome (40).

To date, proteasome inhibitors have been used clinically to treat multiple myeloma and mantle cell lymphoma and are also effective for experimental autoimmune and inflammatory phenotypes, such as arthritis (37) and systemic lupus erythematosus (41). Generally, it is said that proteasome inhibitors induce apoptosis and inhibit immune responses. However, our results indicate that inhibiting the immunoproteasome can induce inflammatory reactions under some circumstances. In this context, the *PSMB8* mutation in NNS can be mimicked by histiocytoid Sweet syndrome (42) and cutaneous vasculitis (43) induced by bortezomib, a nonspecific proteasome inhibitor.

Taken together, the data in the present study suggest that reduction in proteasome activity affects signal transduction and promotes inflammation (Fig. 5). In NNS patients with the *PSMB8* mutation, inflammation causes ubiquitinated proteins to accumulate (compounding the effects on joints, skin, and muscle). These intracellular aggregates may then trigger innate immune responses and increased ROS production (increasing the levels of oxidized proteins), which then, through the activity of p-p38, activate the AP1 transcription factor causing an increase in the secretion of various cytokines such as IL-6.

Materials and Methods

Homozygosity Mapping. The genome-wide ROH overlap pattern was detected using in-house Ruby script (available on request) (44).

Glycerol Density Gradient Separation. Proteins from cell extracts (600 ìg) were separated into 32 fractions by centrifugation (22 h at 100,000 × *g*) in 8 -32 % (vol/vol) linear glycerol gradients.

Additional materials and methods are available in *SI Materials and Methods*.

ACKNOWLEDGMENTS. We thank the families for their participation. We also thank Prof. M. Nakashima for valuable discussion and Ms. C. Hayashida and M. Ohga for technical assistance. This work was supported, in part, by grants from the Ministry of Health, Labour, and Welfare (to F.F., N.K, and K.-i.Y.), the Japan Society for the Promotion of Science (22591094 to H.I., 21390100 to K.-i.Y., 20590331 to A. Kinoshita, 21791566 to H.M., 23791115 to K.A., and 23591651 to N.K.), the Takeda Scientific Foundation and the Naito Foundation (K.i.-Y.), and the Lydia O'Leary Memorial Foundation (N.K.).

1. Nakajo A (1939) Secondary hypertrophic osteoperiostosis with pernio. *J Dermatol Urol* 45:77–86.
2. Nishimura N, Deki T, Kato S (1950) Secondary hypertrophic osteoperiostosis with pernio-like skin lesions observed in two families. *J Dermatol Venereol* 60:136–141.
3. Kitano Y, Matsunaga E, Morimoto T, Okada N, Sano S (1985) A syndrome with nodular erythema, elongated and thickened fingers, and emaciation. *Arch Dermatol* 121: 1053–1056.
4. Tanaka M, et al. (1993) Hereditary lipo-muscular atrophy with joint contracture, skin eruptions and hyper-gamma-globulinemia: A new syndrome. *Intern Med* 32:42–45.
5. Horikoshi A, Iwabuchi S, Iizuka Y, Hagiwara T, Amaki I (1980) A case of partial lipodystrophy with erythema, dactylic deformities, calcification of the basal ganglia, immunological disorders, and low IQ level (Translated from Japanese). *Rinsho Shinkeigaku* 20:173–180.
6. Kasagi S, et al. (2008) A case of periodic-fever-syndrome-like disorder with lipodystrophy, myositis, and autoimmune abnormalities. *Mod Rheumatol* 18:203–207.
7. Oyanagi K, et al. (1987) An autopsy case of a syndrome with muscular atrophy, decreased subcutaneous fat, skin eruption and hyper gamma-globulinemia: Peculiar vascular changes and muscle fiber degeneration. *Acta Neuropathol* 73:313–319.
8. Muramatsu T, Sakamoto K (1987) Secondary hypertrophic osteoperiostosis with pernio (Nakajo). *Skin Res* 29:727–731.
9. Murata S, Yashiroda H, Tanaka K (2009) Molecular mechanisms of proteasome assembly. *Nat Rev Mol Cell Biol* 10:104–115.
10. Jung T, Catalgol B, Grune T (2009) The proteasomal system. *Mol Aspects Med* 30: 191–296.
11. Tanaka K (2009) The proteasome: Overview of structure and functions. *Proc Jpn Acad Ser B Phys Biol Sci* 85:12–36.
12. Fehling HJ, et al. (1994) MHC class I expression in mice lacking the proteasome subunit LMP-7. *Science* 265:1234–1237.
13. Agarwal AK, et al. (2010) PSMB8 encoding the β5i proteasome subunit is mutated in joint contractures, muscle atrophy, microcytic anemia, and panniculitis-induced lipodystrophy syndrome. *Am J Hum Genet* 87:866–872.
14. Garg A, et al. (2010) An autosomal recessive syndrome of joint contracture, muscular atrophy, microcytic anemia, and panniculitis-associated lipodystrophy. *J Clin Endocrinol Metab* 95:E48–E63.
15. Unno M, et al. (2002) The structure of the mammalian 20S proteasome at 2.75 A resolution. *Structure* 10:609–618.
16. Seemuller E, Lupas A, Baumeister W (1996) Autocatalytic processing of the 20S proteasome. *Nature* 382:468–471.
17. Sijts EJAM, Kloetzel P-M (2011) The role of the proteasome in the generation of MHC class I ligands and immune responses. *Cell Mol Life Sci* 68:1491–1502.
18. Hirano Y, et al. (2008) Dissecting beta-ring assembly pathway of the mammalian 20S proteasome. *EMBO J* 27:2204–2213.
19. Hirano Y, et al. (2005) A heterodimeric complex that promotes the assembly of mammalian 20S proteasomes. *Nature* 437:1381–1385.
20. Seifert U, et al. (2010) Immunoproteasomes preserve protein homeostasis upon interferon-induced oxidative stress. *Cell* 142:613–624.
21. Froment C, et al. (2005) A quantitative proteomic approach using two-dimensional gel electrophoresis and isotope-coded affinity tag labeling for studying human 20S proteasome heterogeneity. *Proteomics* 5:2351–2363.
22. Akira S, Taga T, Kishimoto T (1993) Interleukin-6 in biology and medicine. *Adv Immunol* 54:1–78.
23. Kishimoto T (2005) Interleukin-6: From basic science to medicine—40 years in immunology. *Annu Rev Immunol* 23:1–21.
24. Nishimoto N, Kishimoto T (2006) Interleukin 6: From bench to bedside. *Nat Clin Pract Rheumatol* 2:619–626.
25. Gyrd-Hansen M, Meier P (2010) IAPs: From caspase inhibitors to modulators of NF-kappaB, inflammation and cancer. *Nat Rev Cancer* 10:561–574.
26. Pasparakis M (2009) Regulation of tissue homeostasis by NF-kappaB signalling: Implications for inflammatory diseases. *Nat Rev Immunol* 9:778–788.
27. Thalhamer T, McGrath MA, Harnett MM (2008) MAPKs and their relevance to arthritis and inflammation. *Rheumatology (Oxford)* 47:409–414.
28. Kumar S, Boehm J, Lee JC (2003) p38 MAP kinases: Key signalling molecules as therapeutic targets for inflammatory diseases. *Nat Rev Drug Discov* 2:717–726.
29. Kamata H, et al. (2005) Reactive oxygen species promote TNFalpha-induced death and sustained JNK activation by inhibiting MAP kinase phosphatases. *Cell* 120: 649–661.
30. Park GB, et al. (2010) Endoplasmic reticulum stress-mediated apoptosis of EBV-transformed B cells by cross-linking of CD70 is dependent upon generation of reactive oxygen species and activation of p38 MAPK and JNK pathway. *J Immunol* 185: 7274–7284.
31. Villagomez MT, Bae SJ, Ogawa I, Takenaka M, Katayama I (2004) Tumour necrosis factor-α but not interferon-γ is the main inducer of inducible protein-10 in skin fibroblasts from patients with atopic dermatitis. *Br J Dermatol* 150:910–916.
32. Lee EY, Lee Z-H, Song YW (2009) CXCL10 and autoimmune diseases. *Autoimmun Rev* 8:379–383.
33. Dahlqvist J, et al. (2010) A single-nucleotide deletion in the POMP 5′ UTR causes a transcriptional switch and altered epidermal proteasome distribution in KLICK genodermatosis. *Am J Hum Genet* 86:596–603.
34. Caudill CM, et al. (2006) T cells lacking immunoproteasome subunits MECL-1 and LMP7 hyperproliferate in response to polyclonal mitogens. *J Immunol* 176:4075–4082.
35. Hutchinson S, et al. (2011) A dominant role for the immunoproteasome in CD8+ T cell responses to murine cytomegalovirus. *PLoS ONE* 6:e14646.
36. Basler M, Moebius J, Elenich L, Groettrup M, Monaco JJ (2006) An altered T cell repertoire in MECL-1-deficient mice. *J Immunol* 176:6665–6672.
37. Muchamuel T, et al. (2009) A selective inhibitor of the immunoproteasome subunit LMP7 blocks cytokine production and attenuates progression of experimental arthritis. *Nat Med* 15:781–787.
38. Hou N, Torii S, Saito N, Hosaka M, Takeuchi T (2008) Reactive oxygen species-mediated pancreatic beta-cell death is regulated by interactions between stress-activated protein kinases, p38 and c-Jun N-terminal kinase, and mitogen-activated protein kinase phosphatases. *Endocrinology* 149:1654–1665.
39. McCubrey JA, Lahair MM, Franklin RA (2006) Reactive oxygen species-induced activation of the MAP kinase signaling pathways. *Antioxid Redox Signal* 8:1775–1789.
40. Bulua AC, et al. (2011) Mitochondrial reactive oxygen species promote production of proinflammatory cytokines and are elevated in TNFR1-associated periodic syndrome (TRAPS). *J Exp Med* 208:519–533.
41. Neubert K, et al. (2008) The proteasome inhibitor bortezomib depletes plasma cells and protects mice with lupus-like disease from nephritis. *Nat Med* 14:748–755.
42. Murase JE, et al. (2009) Bortezomib-induced histiocytoid Sweet syndrome. *J Am Acad Dermatol* 60:496–497.
43. Gerecitano J, et al. (2006) Drug-induced cutaneous vasculitis in patients with non-Hodgkin lymphoma treated with the novel proteasome inhibitor bortezomib: A possible surrogate marker of response? *Br J Haematol* 134:391–398.
44. Kurotaki N, et al. (2011) Identification of novel schizophrenia Loci by homozygosity mapping using DNA microarray analysis. *PLoS ONE* 6:e20589.

Supporting Information

Arima et al. 10.1073/pnas.1106015108

SI Materials and Methods

DNA and Cell Samples. Genomic DNA was isolated from peripheral blood white cells using a conventional phenol-chloroform method combined with dialysis purification. B cells obtained from peripheral blood were transformed using Epstein-Barr virus.

SNP Genotyping. DNA samples were analyzed using the GeneChip Human Mapping 500K array set (Nsp and Sty arrays) according to the manufacturer's protocol (Affymetrix). Raw array intensity data (CEL files) of 8 of our samples and International HapMap Project phase II Japanese (JPT) samples (n = 45) were genotyped simultaneously using BRLMM genotyping software.

SNP Microarray-Based Homozygosity Mapping. To detect the genome-wide structure of ROHs, SNP genotype files (CHP files) were analyzed using the "unpaired LOH detection" function in the Partek Genomics Suite (GS). To obtain maximum resolution for ROH detection, no SNP heterozygosity baseline files were used. We adopted the following thresholds for ROH: 1.0 Mb for first-cousin marriage offspring (patients 2 and 4), 750 kb for other consanguineous marriage offspring (patients 1 and 3), and 500 kb for nonconsanguineous marriage offspring (patient 5). No filtration was used for the unaffected siblings of patient 4. The genome-wide ROH overlap pattern was detected using in-house Ruby script (1) (available on request) and visualized using Partek GS. A region showing ROHs for all of the patients, but not the unaffected siblings, was considered to be a candidate region.

Mutation Search and Sequencing. All PCR reactions used genomic DNA with KOD FX (Toyobo) or ExTaq DNA polymerase HS (Takara) at the appropriate annealing temperature. PCR products were purified for direct sequencing using Exonuclease I (Epicentre) and shrimp alkaline phosphatase (GE Healthcare). Sequencing reactions used a BigDye Terminator v3.1 Cycle Sequencing kit (Applied Biosystems) and electrophoresed using Autosequencer Model 3130xl.

Structural Modeling. Structural models of mutated and nonmutated immunoproteasomes were constructed by exchanging the residues from the constitutive subunits (2) with those from the inducible subunits. Several of the generated models that had minimum energies were further subjected to an experimental data-free energy minimization process using a Crystallography and NMR system (3).

Cell Culture. LCLs and skin fibroblasts were cultured in RPMI 1640 and DMEM, respectively, supplemented with 10% FBS, 100 IU/mL penicillin G, and 100 mg/mL streptomycin.

Protein Extracts, Immunological Analysis, and Antibodies. Cells were lysed in ice-cold lysis buffer [50 mM Tris-HCl (pH 7.5), 0.5% (vol/vol) Nonidet P-40, and 1 mM DTT with 2 mM ATP and 5 mM $MgCl_2$]. The extracts were clarified by centrifugation at 20,000 × g for 10 min at 4 °C. The supernatants were subjected to SDS/PAGE (12.5% for proteasome subunits or 7.5% for polyubiquitinated proteins) or analyzed by glycerol gradient centrifugation. The separated proteins were transferred onto a polyvinylidene difluoride membrane and incubated with the indicated antibodies. Membranes were developed using the ECL Plus Western Blotting Detection system (GE Healthcare).

Antibodies against proteasome β1, β2, β5, β7, β1i, β2i, and β5i subunits and hUmp-1 were raised in rabbits using recombinant proteins (4). An anti-β4 subunit monoclonal antibody (mAb), anti-Rpt6 mAb, and anti-α6 subunit mAb (MCP20) were purchased from ENZO. An antiubiquitin antibody (Dako), anti–K48- and anti–K63-linked ubiquitin antibodies (Millipore) (4), horseradish peroxidase (HRP)-conjugated antimouse, and antirabbit IgG antibodies (Jackson ImmunoResearch Laboratories) were used for Western blot analysis.

Glycerol Density Gradient Separation. Proteins from cell extracts (600 μg) were separated into 32 fractions by centrifugation (22 h at 100,000 × g) in 8–32% (vol/vol) linear gradients as described previously (6).

Assays for Proteasome Peptidase Activities. Chymotrypsin-like, trypsin-like, and caspase-like activities were determined using the fluorescent peptide substrates succinyl-Leu-Leu-Val-Tyr-7-amido-4-methylcoumarin (Suc-LLVY-MCA), butyloxycarbonyl-Leu-Arg-Arg-4-metylcoumarin (Boc-LRR-MCA), and benzyloxycarbonyl-Leu-Leu-Glu-methylcoumarylamine (Z-LLE-MCA), as described previously (7). The assays for chymotrypsin-like and caspase-like activities were carried out in the presence of 0.03% SDS, which is a potent artificial activator of the latent 20S proteasome.

Assays for Proteolytic Degradation in Vitro. Degradation of the recombinant 35S-labeled ornithine decarboxylase (ODC) was assayed in the presence of ATP, at 20 min and 40 min, as described previously (8). Data were shown in ^{35}S-ODC degradation (%).

Oxidized Protein Detection. Oxidized proteins were visualized using an OxyBlot protein oxidization detection kit (Millipore) following the supplier's protocol.

Immunohistochemistry. Immunohistochemistry used a standard indirect immunofluorescence method. Sections of formalin-fixed, paraffin-embedded tissues were deparaffinized and microwave epitope retrieval was performed after pretreatment at 80 °C for 30 min in 10 mM citrate buffer (pH 6.0). Endogenous peroxidase was inactivated with a 3% H_2O_2 solution following epitope retrieval. After blocking in 5% normal horse serum in PBS, the slides were incubated for 60 min at room temperature with rabbit polyclonal antiubiquitin antibodies (Dako) or a mouse monoclonal antihuman CD68 antibody (ProSci).

Sections were then incubated with FITC-conjugated donkey antimouse IgG or tetramethylrhodamine isothiocyanate-conjugated donkey antirabbit IgG (Jackson ImmunoResearch) in 5% normal horse serum in PBS for 30–45 min at room temperature. After washing in PBS, the slides were mounted in Vectashield mounting medium (Vector Laboratories) and scanned by confocal microscopy (LSM5, PASCAL; Carl Zeiss). Control experiments were performed to ensure the isotype specificity for each of the secondary antibodies. Negative control studies used species-specific IgG as primary antibodies.

Electrophoretic Mobility Shift Assay (EMSA) Using NF-κB Consensus Oligonucleotides. Nuclear proteins were extracted using a Nuclear Extract kit (Active Motif). Nuclear extracts (4 μg) were used for the EMSA assay using an EMSA kit (Pierce). The consensus oligonucleotide sequences for the NF-κB binding motif were: 5′-AGT TGA GGG GAC TTT CCC AGG C-3′ (sense) and 5′-GCCTGGGAAAGTCCCCTCAACT-3′ (antisense). For the competition assay, a nuclear extract was preincubated with an unlabeled oligonucleotide followed by addition of a [γ-^{32}P]-ATP labeled NF-κB probe. Samples were loaded onto 4% polyacrylamide gels (38:1) in 0.5 × TBE and run at 1 W at room

temperature. Gels were dried and exposed to a Storage Phosphor Screen BAS-IP (GE Healthcare). To confirm the integrity of NF-κB binding, anti-p65 and anti-p50 (Santa Cruz Biotechnology) antibodies were used for the supershift assay.

1. Kurotaki N, et al. (2011) Identification of novel schizophrenia Loci by homozygosity mapping using microarray analysis. *PLoS ONE* 6:e20589.
2. Unno M, et al. (2002) The structure of the mammalian 20S proteasome at 2.75 A resolution. *Structure* 10:609–618.
3. Brünger AT, et al. (1998) Crystallography & NMR system: A new software suite for macromolecular structure determination. *Acta Crystallogr D Biol Crystallogr* 54: 905–921.
4. Hirano Y, et al. (2008) Dissecting beta-ring assembly pathway of the mammalian 20S proteasome. *EMBO J* 27:2204–2213.
5. Newton K, et al. (2008) Ubiquitin chain editing revealed by polyubiquitin linkage-specific antibodies. *Cell* 134:668–678.
6. Hirano Y, Murata S, Tanaka K (2005) Large- and small-scale purification of mammalian 26S proteasomes. *Methods Enzymol* 399:227–240.
7. Murata S, et al. (2007) Regulation of CD8+ T cell development by thymus-specific proteasomes. *Science* 316:1349–1353.
8. Hirano Y, et al. (2005) A heterodimeric complex that promotes the assembly of mammalian 20S proteasomes. *Nature* 437:1381–1385.
9. Feng DF, Doolittle RF (1987) Progressive sequence alignment as a prerequisite to correct phylogenetic trees. *J Mol Evol* 25:351–360.

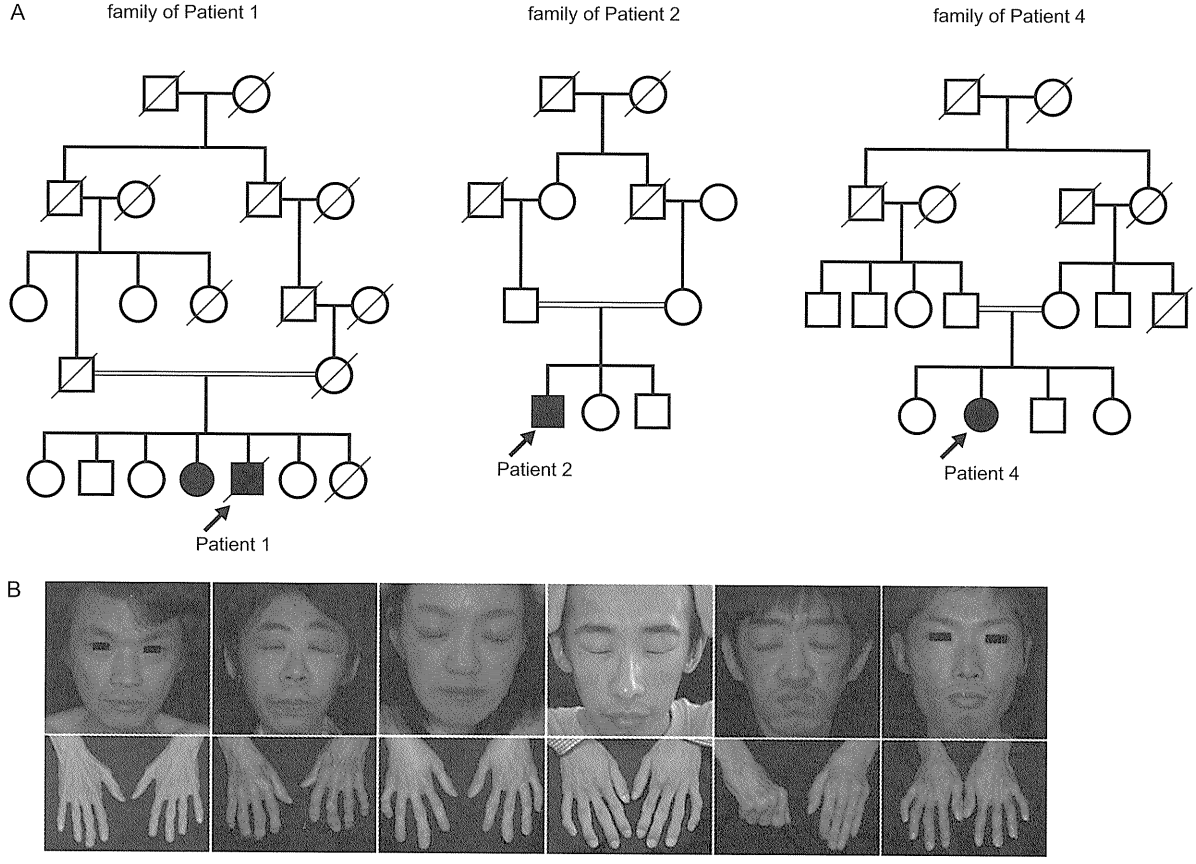

Fig. S1. (Continued)

C

	Patient 1	Patient 2	Patient 3	Patient 4	Patient 5	Patient 6	Patient 7	patient's father	Control 1	Control 2	Control 3	Control 4	Control 5	Control 6	Control 7
rs2857103	TT	TT	TT	TT	TT	TT	TT	TT	TT	GG	GT	GG	GG	GT	TT
rs10484565	GG	GG	GG	GG	GG	GG	GG	GG	AG	AG	GG	GG	GG	GG	GG
rs4148876	GG	GG	GG	GG	GG	GG	GG	GG	GA	AA	GA	AA	AA	GG	GG
rs241439	AA	AA	AA	AA	AA	AA	AA	AA	AA	AA	AA	AC	AC	AC	AA
rs241439	CC	CC	CC	CC	CC	CC	CC	CC	AC	AC	AC	AC	AA	AC	CC
rs241433	GG	GG	GG	GG	GG	GG	GG	GA	GA	GG	AA	GG	GA	GG	GA
rs241433	TT	TT	TT	TT	TT	TT	TT	TT	TT	GT	TT	GG	GT	GT	TT
rs4148872	GG	GG	GG	GG	GG	GG	GG	GG	GG	GG	GG	GG	GG	GA	GG
rs241429	CC	CC	CC	CC	CC	CC	CC	CC	CC	TC	CC	TT	TC	TC	CC
rs3819717	TT	TT	TT	TT	TT	TT	TT	TC	TC	TC	CC	TT	TC	TT	TC
rs241425	TT	TT	TT	TT	TT	TT	TT	TC	TC	CC	TT	CC	TC	TC	TT
rs4148870	AA	AA	AA	AA	AA	AA	AA	AA	GA	GA	GA	AA	GA	GA	GG
rs4713598	TT	TT	TT	TT	TT	TT	TT	TG	TG	TG	TT	GG	TG	TG	TT
rs3763366	CC	CC	CC	CC	CC	CC	CC	CC	CG	CG	GG	CC	CG	CG	GG
rs3763364	TT	TT	TT	TT	TT	TT	TT	TA	TT	TT	TT	AA	TT	TT	TT
rs3763349	CC	CC	CC	CC	CC	CC	CC	CC	TC	TC	TT	CC	TC	TC	TT
PSMB8 exon 5	TT	TT	TT	TT	TT	TT	TT	TG	GG	GG	GG	GG	GG	GG	GG
rs9357155	GG	GG	GG	GG	GG	GG	GG	GA	GA	GG	GG	GG	GG	GG	GG
rs9276810	GG	GG	GG	GG	GG	GG	GG	GA	GA	GG	GG	AA	GA	GA	GG
rs6924102	AA	AA	AA	AA	AA	AA	AA	AG	AG	AG	AA	GG	AG	AG	AA
rs4713599	CC	CC	CC	CC	CC	CC	CC	CA	AA	AA	AA	AA	AA	AA	AA
rs2071543	CC	CC	CC	CC	CC	CC	CC	CA	CA	CC	CC	CC	CC	CC	CC
rs2071463	GG	GG	GG	GG	GG	GG	GG	GG	AG	GG	AA	GG	AG	GG	AG
rs2071541	CC	CC	CC	CC	CC	CC	CC	CT	TT	CT	TT	TT	TT	TT	TT
rs2071540	GG	GG	GG	GG	GG	GG	GG	GG	AG	GG	AA	GG	AG	AG	AA
rs1057373	TT	TT	TT	TT	TT	TT	TT	TG	GG	TG	GG	GG	GG	GG	GG
rs4711312	GG	GG	GG	GG	GG	GG	GG	GA	AA	GA	AA	AA	AA	AA	AA
rs735883	CC	CC	CC	CC	CC	CC	CC	CT	CT	CT	CC	TT	CT	CT	CC
rs2071482	TT	TT	TT	TT	TT	TT	TT	TG	GG	TG	GG	GG	GG	GG	GG
rs4148882	TT	TT	TT	TT	TT	TT	TT	TT	TC	TT	CC	TT	TC	TC	CC
rs12527715	CC	CC	CC	CC	CC	CC	CC	CT	TT	CT	TT	TT	TT	TT	TT
rs12529313	GG	GG	GG	GG	GG	GG	GG	GA	AA	GA	AA	AA	AA	AA	AA
rs2395269	GG	GG	GG	GG	GG	GG	GG	GT	TT	GT	TT	TT	TT		
rs2071538	CC	CC	CC	CC	CC	CC	CC	CC	CC	CC	TC	CC	TC	TC	TC
rs4148880	GG	GG	GG	GG	GG	GG	GG	GA	AA	GA	AA	AA	AA	AA	AA
rs1351383	GG	GG	GG	GG	GG	GG	GG	GT	TT	GG	TT	GG	GT	GT	TT

Fig. S1. (Continued)

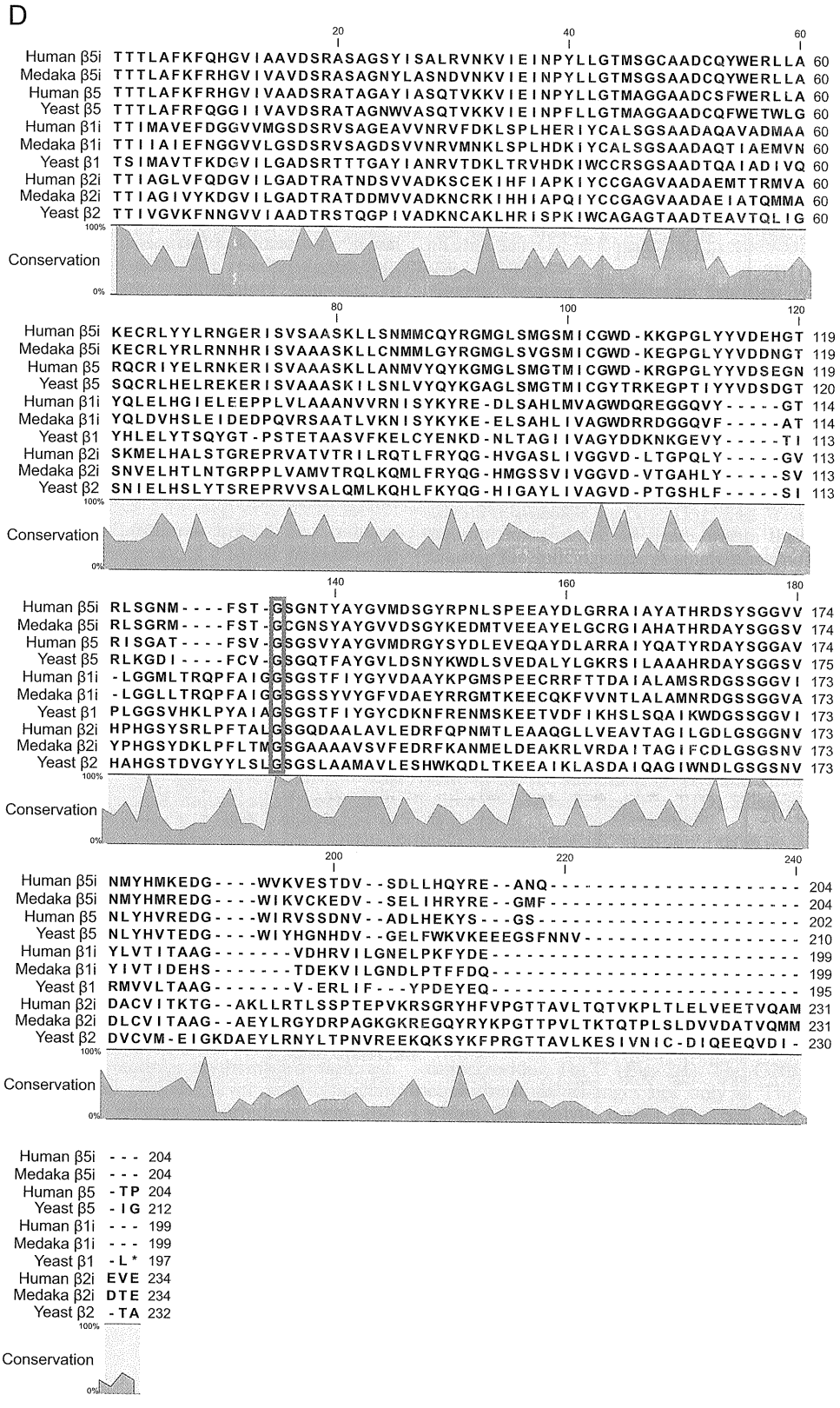

Fig. S1. NNS patients and their consanguineous family histories. (*A*) The families of patients 1, 2, and 4 contain offspring from consanguineous marriages. Solid circles and squares indicate patients with NNS. Arrows, double lines, and diagonal lines indicate probands, consanguineous marriages, and deceased individuals, respectively. (*B*) Photograph of the characteristic thin facial appearance and elongated clubbed fingers in patients 2–7. (*C*) Haplotypes around the *PSMB8* gene mutation. SNPs around *PSMB8* exon 5 were genotyped for seven NNS patients, the father of one patient, and nine controls. All patients shared the same haplotype within this region, which suggests that this mutation was transmitted from a single founder. Control: healthy control in general population. (*D*) Evolutionary conservation of proteasome subunits β5i, β5, β1i, β1, β2i, and β2. Each amino acid sequence is shown in its mature form. The red box indicates the position of the NNS mutation. Multiple amino acid sequence alignment using CLC Sequence Viewer version 6.4, implementing the progressive alignment algorithm (9).

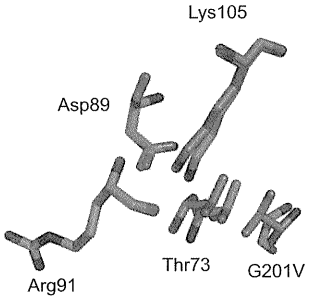

Fig. S2. Computer modeling of mutant β5i. The catalytic residues of proteasome β5i^{G201V} and β5i subunits. Thr73 is the most important catalytic residue within the N terminus of mature β5i. Only the amino acid side chains are shown. Nitrogen and oxygen atoms are blue and red, respectively. The G201V structure is shown in orange and the wild type is shown in green.

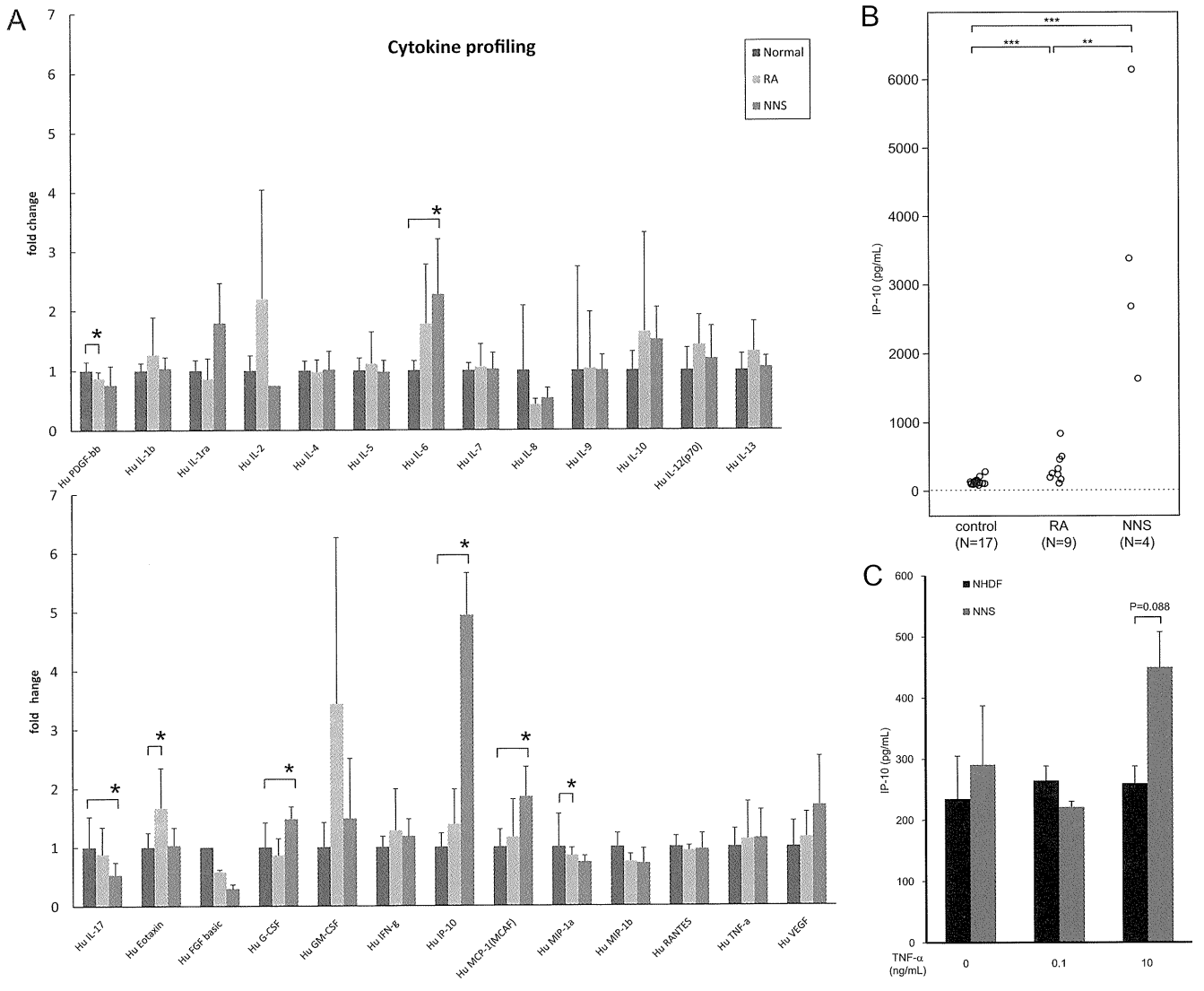

Fig. S3. Cytokine profiles in sera and conditional media from cultured fibroblasts. (*A*) Serum samples were obtained from healthy controls (n = 16), rheumatoid arthritis patients (RA; n = 10), and NNS patients (n = 4). The concentrations of 27 different cytokines were determined using a multiplex bead-based ELISA on a suspension array. Error bars indicate SD of the mean. P values were calculated using two-tailed Welch's t test. *$P \leq 0.05$. (*B*) IP-10 concentration in sera from patients with NNS and RA. IP-10 levels in sera were determined by ELISA on a suspension array. **$P \leq 0.01$, ***$P \leq 0.001$; Mann-Whitney u test. (*C*) IP-10 production by cultured fibroblasts. The concentrations of IP-10 in conditioned media were determined by ELISA (R&D Systems) using triplicate measurements. P, two-tailed Welch's t test.

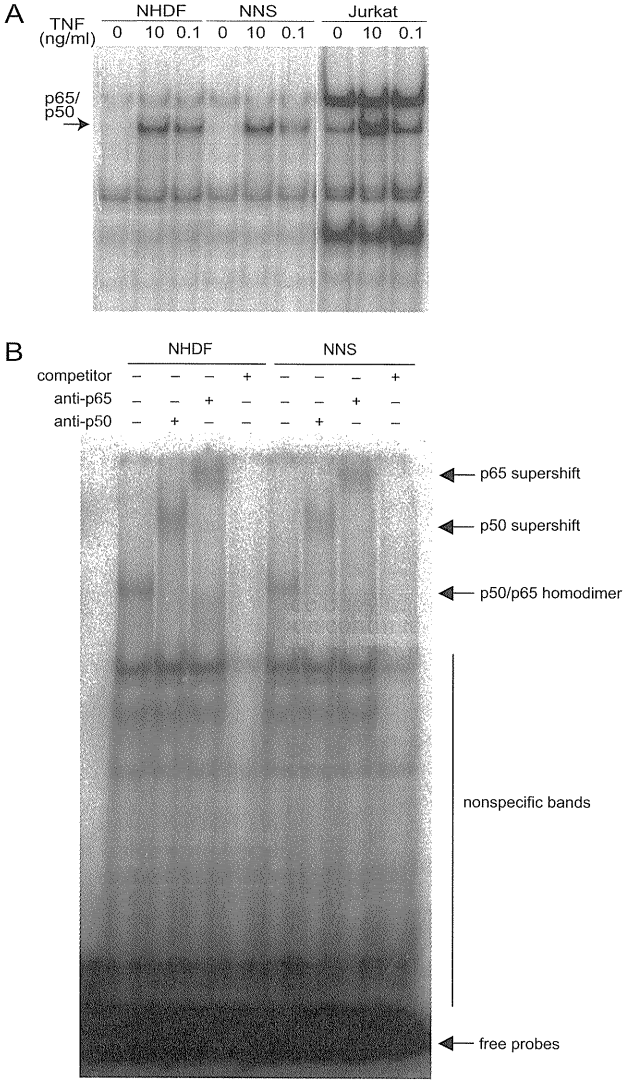

Fig. S4. NF-κB activity in fibroblasts from a NNS patient. (*A*) EMSA for NF-κB. EMSA with an NF-κB consensus probe was performed using nuclear extracts from normal human dermal fibroblast (NHDF), NNS fibroblasts, and Jurkat cells. The NF-κB signal was activated by TNF-α (10 ng/mL or 0.1 ng/mL) in all cell lines. (*B*) EMSA, using a specific antibody, was performed on nuclear extracts from NHDF and NNS after stimulation with TNF-α (10 ng/mL). The signal derived from the p50/p65 heterodimer was confirmed as a supershifted signal in both p50 and p65.

Table S1. Clinical features of our NNS patients compared to JMP syndrome

Patient	1	2	3	4	5	6	7	JMP (3 cases)
Present age, y (at death)	(47)	37	38	31	35	33	32	26–35
Sex	M	M	M	F	M	M	M	M/F
Parental consanguinity	+	+	–	+	–	–	–	–
Family history	+	–	–	–	–	–	–	±
Age at onset of pernio-like rash	–	2 mo	3 mo	6 mo	2 y	1 y	Infancy	–
Heliotrope-like periorbital rash	–	–	+	+	+	+	–	–
Nodular erythema-like eruptions	+	+	+	+	+	+	+	+
Age at onset of fever	12 y	Infancy	7 y	11 mo	2 y	2 y 4 mo	–	–
Partial lipomuscular atrophy	++	+	+	+	+	++	+	+
Long clubbed fingers	+	+	+	+	+	+	+	+
Joint contractures	++	–	+	+	+	++	+	++
Hyperhidrosis	–	+	+	++	–	–	+	NA
Short stature	–	–	–	–	–	+	–	+
Seizures	–	–	–	–	–	–	–	+
Low IQ	+	–	–	–	–	–	–	–
Microcytic anemia	–	+	+	+	+	+	+	+
Elevated ESR/CRP	+	+	+	+	+	+	+	+
High serum CPK	–	+	+	+	–	+	–	+
Hyper-γ-globulinemia	+	+	+	++	+	+	+	+
Antinuclear antibody titer	<40	<40	160	640	80	40	40	–
Positive autoantibody	–	–	MPO-ANCA	dsDNA	SS-A	dsDNA	–	–
Diabetes	+	–	–	–	–	–	–	–
Hypertriglyceridemia	–	–	–	+	+	+	+	–
Low HDL cholesterol	NA	+	–	+	+	+	+	+
Hepatosplenomegaly	+	NA	+	+	+	+	NA	+
Basal ganglia calcification	–	+	+	+	+	+	+	+
Reference	1, 2	3		4				5

All NNS patients have a c.602G > T mutation. M, male; F, female; y, years; mo, months; NA, not assessed; MPO, myeloperoxidase; ANCA, antineutrophil cytoplasmic antibody; ds, double stranded; JMP, joint contracture, muscular atrophy, microcytic anemia, and panniculitis-induced lipodystrophy.

1. Tanaka M, et al. (1993) Hereditary lipo-muscular atrophy with joint contracture, skin eruptions and hyper-gamma-globulinemia: A new syndrome. *Intern Med* 32:42–45.
2. Oyanagi K, et al. (1987) An autopsy case of a syndrome with muscular atrophy, decreased subcutaneous fat, skin eruption and hyper gamma-globulinemia: Peculiar vascular changes and muscle fiber degeneration. *Acta Neuropathol* 73:313–319.
3. Muramatsu T, Sakamoto K (1987) Secondary hypertrophic osteoperiostosis with pernio (Nakajo). *Skin Res* 29:727–731.
4. Kasagi S, et al. (2008) A case of periodic-fever-syndrome-like disorder with lipodystrophy, myositis, and autoimmune abnormalities. *Mod Rheumatol* 18:203–207.
5. Garg A, et al. (2010) An autosomal recessive syndrome of joint contracture, muscular atrophy, microcytic anemia, and panniculitis-associated lipodystrophy. *J Clin Endocrinol Metab* 95: E48–E63.

特集：自己炎症疾患の新しい知見
総　説

中條—西村症候群

金澤伸雄[*1]，有馬和彦[*2]，井田弘明[*3]，吉浦孝一郎[*4]，古川福実[*1]

Nakajo-Nishimura Syndrome

Nobuo KANAZAWA[*1], Kazuhiko ARIMA[*2], Hiroaki IDA[*3], Koh-ichiro YOSHIURA[*4] and Fukumi FURUKAWA[*1]

[*1]*Department of Dermatology, Wakayama Medical University,*
[*2]*Department of Molecular Medicine, Graduate School of Biomedical Sciences, Nagasaki University,*
[*3]*Division of Respirology, Neurology and Rheumatology, Department of Medicine, Kurume University,*
[*4]*Department of Human Genetics, Graduate School of Biomedical Sciences, Nagasaki University*

(Received August 1, 2011)

summary

Nakajo-Nishimura syndrome (NNS) (MIM256040, ORPHA2615) is a distinct inherited inflammatory and wasting disease, which usually begins in early infancy with a pernio-like rash. The patients develop periodic high fever and nodular erythema-like eruptions, and gradually progress lipomuscular atrophy in the upper body, mainly the face and the upper extremities, to show the characteristic long clubbed fingers with joint contractures. So far about 30 cases have been reported from Kansai, especially Wakayama and Osaka, Tohoku and Kanto areas. In addition to 10 cases in Kansai area, which have been confirmed to be alive by national surveillance, an infant case has newly been discovered in Wakayama and more cases will be added. Although cause of the disease has long been undefined, a homozygous mutation of the *PSMB8* gene, which encodes the β5i subunit of immunoproteasome, has been identified by homozygosity mapping. By analyses of the patients-derived cells and tissues, it has been suggested that accumulation of ubiquitinated and oxidated proteins due to deficiency of proteasome activities cause hyperactivation of p38 MAPK and overproduction of IL-6. Similar diseases with *PSMB8* mutations have recently been reported from Europe and the U.S.A., and therefore, it is becoming clear that proteasome deficiency syndromes are globally distributed as a new category of the autoinflammatory diseases.

Key words——Nakajo-Nishimura syndrome; lipomuscular atrophy; *PSMB8*; immunoproteasome; ubiquitin

抄　録

中條—西村症候群（ORPHA 2615, MIM 256040）は，幼小児期に凍瘡様皮疹で発症し，弛張熱や結節性紅斑様皮疹を伴いながら，次第に顔面・上肢を中心とした上半身のやせと拘縮を伴う長く節くれだった指趾が明らかになる特異な遺伝性炎症・消耗性疾患である．和歌山，大阪を中心とした関西と東北，関東地方に偏在し，30例近い報告がある．全国疫学調査で生存が確認された関西の10症例に加え，新規幼児例が和歌山で見出され，今後も増える可能性がある．長らく原因不明であったが，ホモ接合マッピングにより，免疫プロテアソームβ5iサブユニットをコードする*PSMB8*遺伝子のホモ変異が同定された．患者由来細胞，組織の検討により，本疾患ではプロテアソーム機能不全のためにユビキチン化，酸化蛋白質が蓄積することによって，p38 MAPK経路が過剰に活性化しIL-6が過剰に産生されることが示唆された．最近，欧米からも*PSMB8*遺伝子変異を伴う類症が報告され，遺伝性自己炎症疾患の新たなカテゴリーであるプロテアソーム不全症が世界に分布することが明らかになりつつある．

I. 疾患の定義・概念

1939年に東北帝国大学医学部皮膚科泌尿器科の中條により，血族婚家系に生じた兄妹例が「凍瘡ヲ合併セル続発性肥大性骨骨膜症」として報告されたのが，本疾患の最初の記載とされる（図1a）[1]．凍瘡と骨膜肥厚を伴うばち状指を特徴とし，心不全に基づく末梢循環障害が原因として想定された．さらに1950年，和歌山県立医科大学皮膚科泌尿器科の西村らは，血族婚の2家系に生じた3症例を報告

[*1]和歌山県立医科大学医学部皮膚科，[*2]長崎大学大学院医歯薬学総合研究科分子医学，[*3]久留米大学医学部呼吸器・神経・膠原病内科，[*4]長崎大学大学院医歯薬学総合研究科人類遺伝学

a

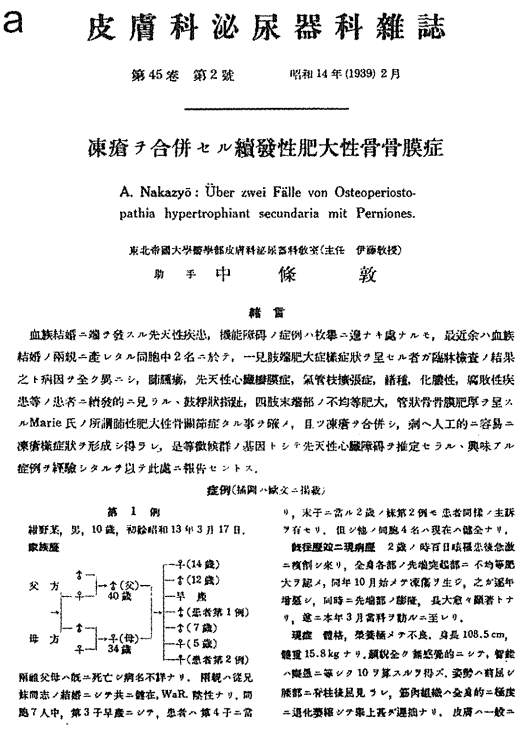

皮膚科泌尿器科雑誌

第45巻 第2號　昭和14年(1939) 2月

凍瘡ヲ合併セル續發性肥大性骨骨膜症

A. Nakazyō: Über zwei Fälle von Osteoperiostopathia hypertrophiant secundaria mit Perniones.

東北帝國大學醫學部皮膚科泌尿器科教室(主任 伊藤教授)

助手 中條敦

抄録

血族結婚ニ續ク發スル先天性疾患，機能障碍ノ症例ハ枚擧ニ遑ナキ處ナルモ，最近余ハ血族結婚ノ兩親ニ產レタル同胞中2名ニ於テ，一見肢端肥大症樣症狀ヲ呈セル者ガ臨牀檢査ノ結果之ト病因ヲ全ク異ニシ，腦腫瘍，先天性心臟機能症，氣管枝擴張症，結核，化膿性，腐敗性疾患等ノ患者ニ續發的ニ見ラル、肢梓狀指症，四肢末端部ノ不均等肥大，管狀骨骨膜肥厚ヲ呈スルMarie氏ノ所謂肺性肥大性骨關節症タル事ヲ確メ，且ツ凍瘡ヲ合併シ，洞ノ人工的ニ容易ニ凍瘡樣症狀ヲ形成シ得ラレ，是等徴候群ノ基因トシテ先天性心臟障碍ヲ推定セラル、興味アル症例ヲ經驗シタルヲ以テ此處ニ報告セントス．

症例(插圖ハ缺文ニ揭載)

第 1 例

禰野某，男，10歲，初診昭和13年3月17日．

家族歷

兩親父母ハ既ニ死亡シ病名不詳ナリ．兩親ハ從兄妹間ノ結婚ニシテ共ニ健在，WaR. 陰性ナリ．同胞7人中，第3子早產ニシテ，患者ハ第4子ニ當リ，次子ニ當ル2歲ノ妹第2例モ患者同樣ノ主訴ヲ有セリ．但シ他ノ同胞4名ハ現在ハ健全ナリ．

既往歷竝ニ現病歷　2歲ノ時百日咳樣患後急激ニ腹脹シ來リ，全身各部ノ先端突起部ニ不均等肥大ヲ起メ，同年10月始メテ凍傷ヲ生ジ，之ガ逐年增惡シ，同時ニ先端部ノ腫痛，長大怠々顧著トナリ，遂ニ本年3月當科ヲ訪ルルニ至レリ．

現症　體格，榮養極メテ不良．身長108.5cm，體重15.8kgナリ．觸覺全ク無痙攣的ニシテ，智能ハ魯鈍ニ等シク10ヲ算スルヲ得ズ．姿勢ハ前屈シ脈管ニ著明ナル見ラレ，筋肉組織ハ全身的ニ極度ニ退化萎縮シテ乘上者ガ選拔ナリ．皮膚ハ一般ニ

b

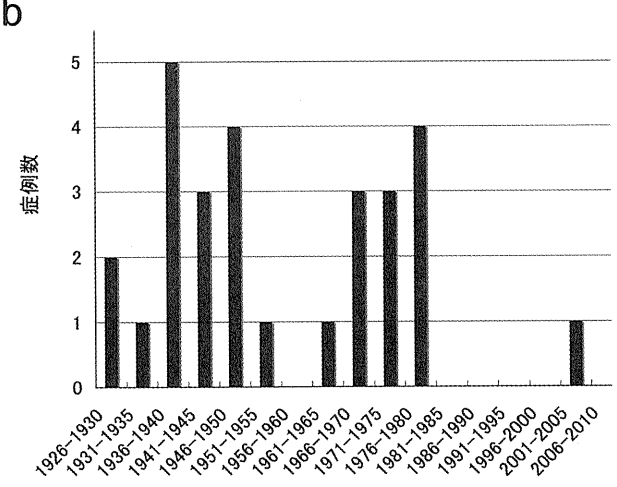

図1　a)1939年の中條の報告．b)本邦28例の生年のまとめ．

し，これが原発性の遺伝性疾患である可能性を指摘した[2]．その後も皮膚科領域から主に関西の症例の報告が続き，1985年，大阪大学（のちに兵庫医科大学）の喜多野らが自験例4症例を含む8家系12症例をまとめ，これまでに報告のない新しい疾患“A syndrome with nodular erythema, elongated and thickened fingers, and emaciation”としてArchives of Dermatology誌に発表した[3~9]．これを受け，国際的な遺伝疾患データベースであるMIMにNakajo syndrome（MIM256040）として，さらに稀少疾患データベースであるORHANETにNakajo syndrome（Nodular erythema-digital changes; ORPHA1953）あるいはNakajo-Nishimura syndrome（Amyotrophy-fat tissue anomaly; ORPHA2615）として登録された．

内科領域においては，西村らの報告例を同大学内科の加藤と神経科の本多が本邦6例目の進行性リポジストロフィー例として報告したのが最初であるが，ほとんど顧みられなかった[10]．1971年に日本大学内科の堀内らによって「皮膚紅斑，筋萎縮，脾腫，γ-グロブリンの上昇，IgAの減少が見られた膠原病類似疾患」の1症例が報告されたのを契機に内科領域でも関心を持たれるようになり，さらに秋田と新潟から2家系3症例が特殊なリポジストロフィーとして報告された[11~14]．1986年にこの疾患が皮膚科領域で報告されてきた疾患と同一であることが指摘されたことを受け，新潟大学神経内科の田中らがそれまでの報告例をまとめ，新しい疾患“Hereditary lipo-muscular atrophy with joint contracture, skin eruptions and hyper-γ-globulinemia”として，1991年に日本医事新報に，さらに1993年にInternal Medicine誌に発表した[15~17]．

小児科領域からは，1985年に高知医科大学の脇口らによって深在性エリテマトーデスとして報告された成人例（大阪出身）があるが，小児例を集めた報告は1986年の和歌山県立医科大学の杉野らの学会報告のみである[18~20]．杉野らは，本疾患における周期性発熱と地域的偏りに着目し，遺伝性自己炎症疾患の代表である家族性地中海熱/Familial Mediterranean fever（FMF）を模して「家族性日本熱/Familial Japanese fever（FJF）」という疾患名を提唱している[21~23]．

このように本邦固有の劣性遺伝性疾患と考えられながら，原因遺伝子は長らく不明であった．2006年に自己炎症疾患を専門とする和歌山県立医科大学皮膚科の金澤と長崎大学（のちに久留米大学）内科の井田がこの疾患の存在に気付き，人類遺伝学の吉浦との共同研究によって，2009年に遂に免疫プロテアソームのサブユニットをコードする*PSMB8*遺伝子のホモ変異が原因であることをつきとめ，本疾

患の本態がプロテアソーム機能不全であることを明らかにした[24]．ほぼ同時期に，徳島大学の安友らも独自に遺伝子変異を同定した[25]．一方，2010年にスペインとアメリカのグループから，それぞれCANDLE症候群とJMP症候群という臨床的に本症と非常に良く似た疾患が報告され，さらにこれらも*PSMB8*遺伝子変異が原因であることが明らかとなり，本症と合わせてプロテアソーム不全症が世界に分布することが明らかになりつつある[26~29]．

II. 疫　　学

本疾患が「中條—西村症候群」との疾患名のもと，本邦固有の稀少難治性疾患として2009年度厚生労働科学研究費補助金難治性疾患克服研究事業の研究奨励分野177疾患の一つに採択されたことを受け，事業の一環として全国疫学調査をおこなった．まず，和歌山県立医科大学皮膚科にて診察した本疾患患者11例のまとめをもとに，特徴的な8症状（血族婚・家族内発症，手足の凍瘡様紫紅色斑，繰り返す弛張熱，出没する浸潤性・硬結性紅斑，進行する限局性脂肪筋肉萎縮・やせ，手足の長く節くれだった指・関節拘縮，肝脾腫，大脳基底核石灰化）を選び，そのうち5つ以上を呈し他疾患を除外できるものを確定例，2つ以上を呈するものを疑い例とする診断基準案を作成した（表1）．典型例の幼児期，成人期の写真をつけた参考資料とともに，全国の大学病院と500床以上の一般大病院の代謝・内分泌・リウマチ・膠原病・神経内科，皮膚科，小児科，整形外科（大学623，病院1193施設）に調査用紙を送布し，過去5年間の有病率調査を行った結果，大学病院371（回答率59.6%）と一般大病院433施設（36.3%）より回答を得たが，既報告例と既に当方に問い合わせのあった症例を除き，確定例，疑い例ともに新規の症例はなかった．

表1　中條—西村症候群診断基準案

1. 常染色体劣性遺伝（血族婚や家族内発症あり）
2. 手足の凍瘡様紫紅色斑（乳幼児期から冬期に出現）
3. 強い浸潤・硬結を伴う結節性紅斑が出没（環状のこともある）
4. 繰り返す弛張熱（周期熱：必発ではない）
5. 手足の長く節くれだった指・関節拘縮
6. 進行性の限局性脂肪筋肉萎縮・やせ（顔面・上肢に著明）
7. 肝脾腫
8. 大脳基底核石灰化

8項目中5項目以上陽性で他疾患を除外できれば確定

既報告・既知例は，東北・関東より5家系7症例（宮城，東京，秋田，新潟），関西より17家系20症例（和歌山，大阪，奈良）あるが，秋田の症例が2009年12月に死亡したのをはじめ，追跡不能な症例が多く，現在もフォローを継続している症例は関西の10症例のみであった（表2：出生地が明らかでない症例については，報告した大学がある県を出身県として記載した）．

一方，300床で今回の調査対象ではなかった和歌山市中病院の皮膚科・小児科にて3年前よりフォローしている5歳の患児が診断基準を満たし，さらに*PSMB8*遺伝子のホモ変異も証明され，約20年ぶりの新規症例であることが判明した．そこで東北と関西の300床以上の病院761施設まで疫学調査の対象を広げて調査を追加したが，やはり新規症例は見いだされなかった．

これら28例の生年を集計すると（一部推定），1940/50年前後，1970/80年前後に集中しており，強い創始者効果によって30年周期に生まれているとすれば，2000/2010年生まれの症例が今後も出現する可能性が想定される（図1b）．

III. 臨床症状

以前の報告に加え，現時点で研究班が把握しているすべての既報告・既知例23家系28例について，特徴的な臨床症状と検査異常の有無を表2にまとめ，また現在和歌山県立医科大学でフォロー中の代表的な女性例（症例20）の臨床写真を図2に示した[30,31]．男女比は19：9と男性が約2倍多く，血族婚あるいは家族歴のあるものが約7割の家系に認められた．1例を除き生後2ヶ月から8歳までの幼小児期に発症し，その多くが凍瘡様紅斑を初発症状としていた．生まれて最初の冬に重症の凍瘡が出現し，毎年繰り返すというケースが典型であり，患者にも医師にも病気としての自覚がないことがある（図2a）[19]．皮疹としては，むしろ赤くやや膨隆し境界明瞭な硬い結節，浸潤性紅斑として触れるいわゆる結節性紅斑が特徴的と考えられ，実際，全例に認められた（図2h）．ただこれも冬期に増悪し，寒冷負荷試験で誘発されうることから，西村らや坂本らのように，このタイプの皮疹を凍瘡様皮疹として報告している場合もある[2,4,7]．いずれも血管障害による炎症性病変という共通の病態と考えられるが，見落とされがちな初発症状として，冬期に指先や耳

表 2a　中條—西村症候群患者の臨床症状のまとめ

症例	年齢	性別	出身県	血族婚	家族歴	発症年齢	凍瘡様紅斑	結節性紅斑	周期熱	リンパ節腫脹	長く節くれた指	関節拘縮	脂肪萎縮	筋萎縮	知能低下	文献
1	10y	M	宮城	+	+	2y	+	+	−	+	+		**X**	+	+	1
2	8m	F	宮城	+	+	7m	**X**	+								1
3	18y	F	和歌山	+	+	5y		**X**			+		+	−		2, 10
4	12y	F	和歌山	+	+	2y		**X**			+		+	+	+	2
5	9y	M	和歌山	+	+	4y		**X**			+		+	+		2
6	23y	F	東京			1–2y	**X**	+			+					3
7	5y	M	奈良	+	−	2y		+			+		**X**	+		4
8	7y	M	大阪	+		3y	**X**	+	+	+	+	+	+	+	−	5
9	37y	M	大阪	+		6m	**X**	+		−	+	+	+	+	−	6
10	7y	M	大阪	+	+	4m	**X**	+		+	+		+		−	6
11	32y	M	大阪	+	+	1y	**X**	+	+	+	+	+	+	+	+	6
12	10y	M	奈良	+	−	2m		**X**	+		+	−	+		−	7, 24
13	11y	M	和歌山	−	−	1y		**X**	−		+	+	+		−	7, 22
14	5y	M	大阪	−	−	2m	+	**X**	+	+	+		+	+	−	9
15	31y	F	東京	−	−	3m	**X**	+	+	−	+	+	+	+	+	11, 12
16	22y	F	秋田	+	±	8y		+	+	+	+	+	**X**	+		13
17	41y	M	新潟	+	+	12y		+	+		**X**	+	+	+	+	14, 15
18	44y	F	新潟	+	+	6y		+	+		**X**	+	+	+	+	14, 15
19	32y	M	大阪	+	±	幼少時	**X**	+	+	−	+	+	+		+	18, 19
20	6y	F	和歌山	+	−	6m	**X**	+	+	−	+	+	+		−	20, 21
21	13y	M	和歌山	−	−	3m	**X**	+	+		+	+	+		−	20, 23
22	18y	F	大阪	+	+	6m	**X**	+	+		+	−	+		−	20, 23
23	17y	M	大阪	+	+	1y10m	**X**	+	+	+	+	−	+		−	20, 23
24	31y	M	大阪	−	−	幼少時	**X**	+	−		+	−	+	−	−	23, 24
25	32y	M	和歌山	−	−	1y	**X**	+	+	+	+	+	+	+	+	23, 24
26	62y	M	和歌山	+	−	6y	+	+	**X**		+	+	+	+	−	23
27	36y	M	大阪	−	−	2y	**X**	+	**X**		+	+	+		−	24
28	5y	M	和歌山	−	−	2m	+	**X**	+		+		+		−	

（注：現在生存が明らかな症例番号の背景を黒色で，診断基準項目の背景を灰色で示す．また，各症例の初発症状を **X** で示した．）

介に生じる典型的な凍瘡と酷似した暗紫紅色の浮腫性紅斑を凍瘡様紅斑とし，結節性紅斑と分けて一項目とした．周期熱は必発ではないが，古い報告もよく読めばさまざまな発熱の記載が見られ，リンパ節腫脹を伴う例もある[5,6,11]．中條の報告例では百日咳が発症の誘因となった可能性があるが，ほかにも中耳炎後に発症した例やサイトメガロウイルス感染が重なった症例がある[1,4]．本疾患において最も特徴的ともいえる長く節くれだった指と顔面，上肢に強い限局性脂肪（筋肉）萎縮はほぼ必発である．成長に伴って徐々に明らかとなるが，これを初発症状とする症例もあり，早期から注意が必要であろう．一方，知能低下を示す症例はわずか 8 例のみであり，本疾患によるものとは考えにくい．このほか眼瞼のヘリオトロープ様紅斑や筋炎（図 2e, i），低身長，掌蹠の多汗症，足底の重度の鶏眼なども報告されている[6,9,21,23]．

IV.　臨床検査所見

赤沈亢進は程度の差はあれ，ほぼすべての症例に認められた．貧血は小球性で鉄欠乏を伴うことが多いが，鉄剤に反応せず，慢性炎症，脾腫に伴うものと考えられる．血小板減少症を伴った例もある[5]．CPK 高値は筋炎に伴うものと考えられ，神経学的検索にて筋原性変化を認める例が多いが，筋萎縮の有無とは必ずしも一致しない．大半の症例に認めるγグロブリン高値も慢性炎症の結果と考えられ，IgG が高値となるが，IgA が低値の例や IgE が異常高値となる例も報告されている[11,12,21]．さらに，発症時に自己抗体が陽性の症例はないものの，経過中に抗核抗体が陽性となり，抗 DNA 抗体をはじめとする自己抗体が検出される例が少なくないことは注目に値する．一方，リンパ球幼弱化試験は正常とされるが，細胞性免疫の指標としてのツベルクリン反応は，少数ながら記載のある報告すべてで陰性であ

表 2b　中條―西村症候群患者の臨床検査異常のまとめ

症例	赤沈亢進	貧血	CPK高値	γグロブリン高値	抗核抗体	自己抗体	ツベルクリン反応	肝脾腫	基底核石灰化	寒冷負荷試験	骨膜肥厚	コレステロール	中性脂肪
1	+	+						+		+	+	H	H
2													
3	+	+		+			−	−	−	−	±		
4	+	+		+				−		−	+		
5	+	+		+				−		+	+		
6													
7	+	+		+				−		−	±	H	
8	+	−		+			−	+		+	−	N	
9	+	+		+						+	−	L	N
10	+	+		+						+	−	L	
11	+	+		−						−	−	L	
12	+	+	+	+	<40	−			+			L	
13	+	+	−	+	80	−		+	+		−	N	N
14	+	+	±	−	160	−				+	−	L	
15	+	+	+	+	+	−	−	+	+			H	H
16	+	+	+	+	−	−		−				N	H
17	+	−	−	+	−	−	−	+	−			L	N
18	+		−	+	−	−	−	+	+			L	N
19	+	−		+	+	DNA		−	+				
20	+	+	+	+	640	dsDNA, SS-B		+	+		−	L	H
21	+	+	+	+	160	MPO-ANCA		+	+		−	L	N
22	+	+	±	+	160	ss, dsDNA		+	+		−	N	H
23	+	+	±	+	2560	SS-A		+	+		−	H	H
24	+	+	−	+	40	−			+		−	L	H
25	+	+	+	+	40	dsDNA		+	+		−	H	H
26	+	+	−	−	+	−		+	+		−	H	N
27	+	+	−	+	80	SS-A		+	+	−	−	L	H
28	+	+	−	−	<40	−		+	+		−	N	N

（注：H：高値，N：正常値，L：低値）

った．NK 活性については，3 例に著明な低下を認めた一方で，活性は高値あるいは正常で細胞数が箸増していたという報告もあり，更なる検討が必要である[15,18,19,21]．臓器病変としては，肝脾腫と大脳基底核石灰化を多くの症例に認めた．特に大脳基底核石灰化は特異度が高いと考えられ，本疾患を疑った場合は積極的に検索する必要がある．一方，初期に本疾患の特徴的所見と考えられた骨膜肥厚は，その後の報告ではほとんど認められていない．特徴的な節くれだった外観に対し，レントゲン上は骨融解像や関節裂隙の狭小化を認めず，血中 MMP-3 値も正常である．寒冷負荷試験は中條が記載したもので，4℃ の冷水に 15 分間両手をつけると，5 時間後に前腕の表在血管の走行に沿って凍瘡様結節性紅斑が出現したというものである[1]．西村らも，冷水負荷の 4 時間後に前腕の血管に沿った結節の新生と従来の結節の発赤腫脹の増悪，さらに全身の蕁麻疹様発疹が出現したと報告した[2]．一方，橋本と喜多野は冷水負荷の 24 時間後あるいは翌日に結節，紅斑が新生したと報告している[5,6]．陽性率は高くないが，本症の発症メカニズムを探る上で重要な検査と考えられる．血中サイトカイン濃度の検討では，IL-1β と TNFα は健常者と変わりなく，複数の患者に共通して有意に高いのは IL-6 とケモカインの IP-10 であった[21,24]．大脳基底核石灰化や全身性エリテマトーデスと関連が深いとされる IFN-α についても，今後検討が必要であろう[32]．脂肪萎縮に関連して血清脂質が測定されているが，中性脂肪が高い例が多いのに対し，総コレステロール値には一定した傾向は認められなかった．今後は，むしろレプチンやアディポネクチンなど脂肪細胞が産生する，あるいはそれらに働く生理活性物質の検討が必要であろう[33]．このほか，心電図にて様々な程度に伝導障害や虚血性変化を認めることが多く，早世あるいは突然死の一つの要因と考えられる．内分泌学的検索で明らかな異常を認めることはほとんどないが，症例

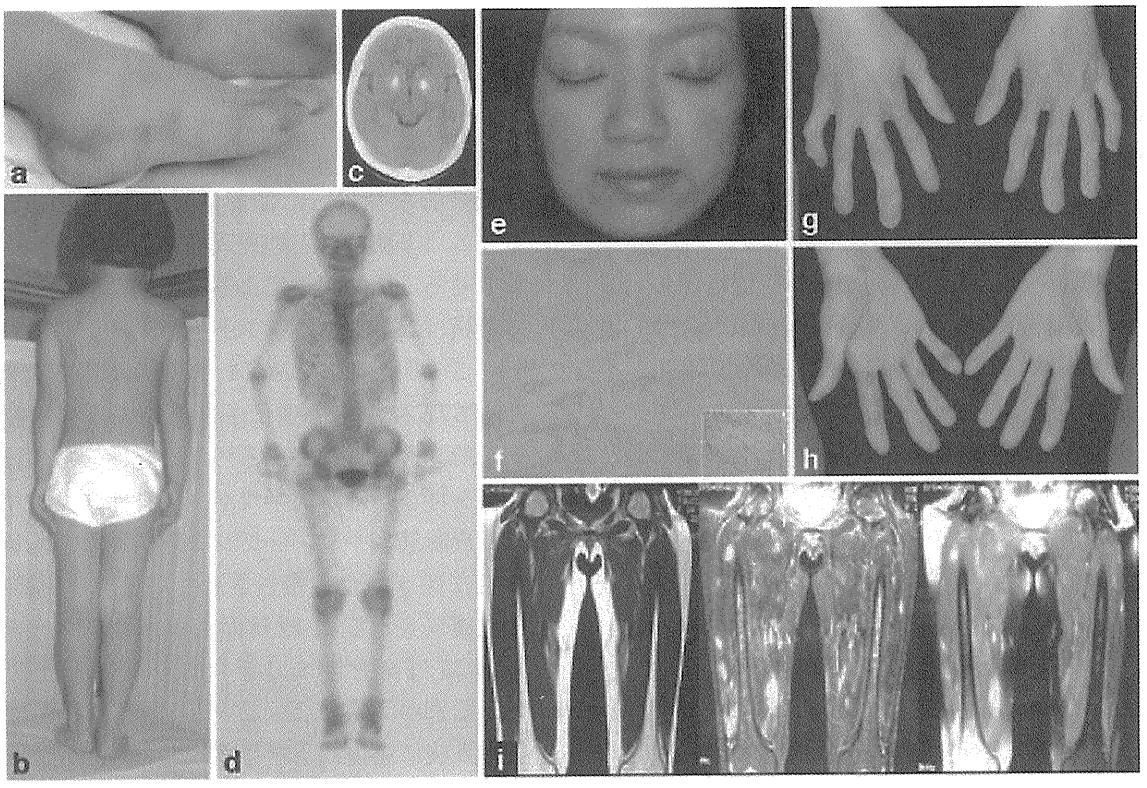

図 2　症例 20 の臨床像

a）右足外側縁の凍瘡様紅斑（5 歳時）．b）下腿筋炎による尖足位．c）CT での大脳基底核石灰化（24 歳時）．d）骨シンチにおける関節部異常集積像．e）ヘリオロープ様眼瞼紅斑を伴うやせて骨ばった顔貌（27 歳時）．f）手掌の結節性紅斑様皮疹の病理組織像．g）長く節くれだった指．h）右手首，左手掌に結節性紅斑様皮疹を認める．i）大腿筋の MRI 像（左より T1, T2，ガドリニウム強調 T1 像．24 歳時）

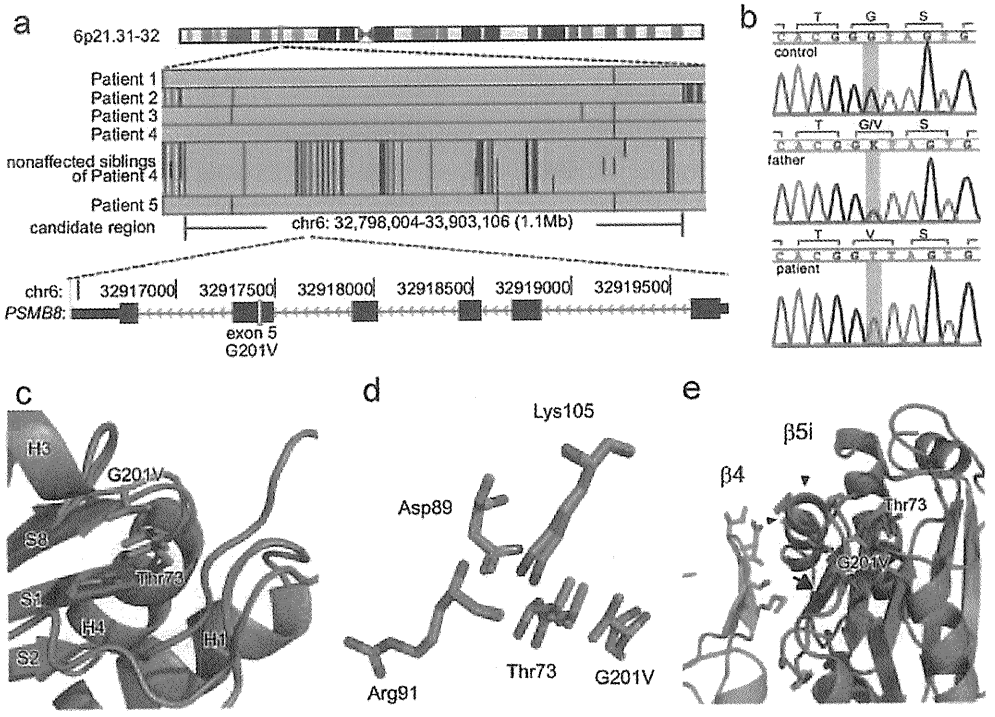

図 3　中條—西村症候群の責任遺伝子の同定

a）患者 5 人とその兄弟 3 人のゲノムを用いたホモ接合マッピング．緑の縦線は SNP のヘテロ接合を表す．b）*PSMB8* 遺伝子の 602 番目（黄線）を中心とした遺伝子波形．c）β5i サブユニットの立体構造モデルの拡大像．緑：野生型，橙：G201V 変異型．S：β シート，H：α ヘリックス．d）G201V 変異による活性中心の構造変化．e）G201V 変異による β4 との接合面の変化．矢印は β シート，矢頭は S8 と H3 のループを示す．

25のように低身長で成長ホルモンを投与された例もある[23]．ガリウムシンチ，骨シンチ（図2d）やPET, MRI（図2i）にて骨，関節，筋肉内の炎症病巣を検索した例もある[21]．

V. 病理検査所見

凍瘡様あるいは結節性紅斑様皮疹の生検では，真皮全層から脂肪織，場合によっては筋層に至るまで巣状に血管周囲あるいは付属器，特に汗腺周囲に超密な炎症細胞浸潤を認める．浸潤細胞はリンパ球，組織球が主体で，核破砕を伴う好中球や好酸球の浸潤を認める例もある．フィブリノイド壊死を伴う明らかな血管炎を認めることはなく，むしろ内皮細胞の増殖と硝子様物質の沈着を伴う壁の肥厚による内腔の狭窄を認める（図2f）．浸潤細胞に軽度の異型を認めることもあるが，CD4, CD8, CD68，ミエロペルオキシターゼ陽性細胞をはじめ多彩な細胞が浸潤し，モノクロナリティは認めない[34]．

47才にて心不全で死亡した症例17の剖検結果によると，萎縮した骨格筋に束状の線維化を散在性に認め，残った筋肉内にもrimmed vacuole（縁取り空泡）や小葉化した筋線維を多数認めた[35]．電顕的にも筋線維の壊死，増加したミトコンドリア内や細胞質内に封入体を認めたが，末梢神経や神経筋接合部には問題なく，再生線維や炎症細胞浸潤も認められなかった．同様の変化は舌や外眼筋，心筋にも認めた．一方，萎縮の強い小葉に限って，動静脈から毛細血管に至るまで，内皮細胞の肥厚あるいは平滑筋細胞の増生，間質の増加，壊死した内皮細胞の破砕物によって，内腔の狭小化あるいは閉塞像を認めた．内皮細胞中に増加したWeibel-Palade小体を認める一方，内弾性板断裂やフィブリン析出，動脈硬化やウイルス封入体，炎症細胞浸潤は認めなかった．また大脳の石灰化を認めた部位に一致して，小血管にカルシウム沈着を認めたが，視床下部，皮質脊髄路，脊髄前角細胞や脊髄神経根には異常を認めなかった．肝臓は中心性脂肪変性を認め，脾臓は鬱血していた．皮下脂肪の減少に対して臓器周囲の脂肪は増えていたが，脂肪細胞そのものには電顕的に明らかな異常は認められなかった．その後，新潟から秋田に移った豊島と山田らによって，症例16の筋生検組織と38歳にて肺炎で死亡した症例15の剖検検体が検討され，前者にて症例17と同様の多数のrimmed vacuoleが認められたものの明らかな血管病変はなく，また後者においても肋間筋に空泡を含む萎縮筋線維が認められたのみで，血管病変は認められなかった[36,37]．

VI. 診断，鑑別診断

特徴的な骨張った顔貌はガーゴイル様とも称され，ムコ多糖症などの先天性代謝異常症の存在を想起させる．脂肪萎縮による特徴的な顔貌と節くれだった指は限局性リポジストロフィーそのものであるが，この疾患には*LMNA*, *PPARγ*, *AKT2*, *CIDEC*, *ZMPSTE24*などの遺伝子変異による家族性のものと，続発性のものがある[33]．続発性のものは低補体血症を伴うものが大半だが，全身性エリテマトーデス，皮膚筋炎やシェーグレン症候群などの自己免疫疾患に伴う場合も報告されている[38]．実際症例15は皮膚筋炎，症例19は深在性エリテマトーデス，症例25は全身性エリテマトーデスと当初考えられ，鑑別が問題となった[11,12,18,19,23]．症例25はさらに成人後に筋力低下を伴う筋炎を発症し，筋生検の病理所見より封入体筋炎と診断されたが，症例17の剖検所見を鑑みても，組織学的鑑別は困難と思われる．また乳幼児期から凍瘡と大脳基底核石灰化を呈する疾患として，*TREX1*などのエンドヌクレアーゼ遺伝子の変異によるAicardi-Goutieres症候群（家族性凍瘡様ループス）も鑑別に挙げられる[32]．進行性の脂肪萎縮や重度の鶏眼は早老症であるWerner症候群も想起させるが，早期発症の白内障や白髪は認めない．

一方，発熱を伴う結節性紅斑を繰り返し，脂肪貪食を伴う小葉性脂肪織炎によって治癒後に陥凹を残す疾患にWeber-Christian病があり，実際症例22と23は当初そう診断された．稀ではあるが，α1-アンチトリプシン/α1-アンチキモトリプシン欠損症も脂肪織炎による結節性紅斑を生じる．中條—西村症候群では，脂肪織炎を繰り返すことで陥凹が増えてやせるというよりも，末梢から系統的にやせていくのが特徴である．ただWeber-Christian病の診断には他疾患の除外が必要であり，むしろ積極的に中條—西村症候群かどうか判断する必要がある．先にあげた臨床診断基準案によると，症例1と症例7以降の23症例すべてで診断基準8項目中5項目以上を満たすが，症状が完成する前の早期診断が可能か，また疾患特異性について，偽陽性となる疾患がないかなど，今後も検討を要する．

寒冷で誘発され，一定しない熱型，骨張った顔貌などの共通点から，周期熱を伴う自己炎症疾患の中

表3 プロテアソーム不全症3疾患の比較

	中條—西村症候群	JMP症候群	CANDLE症候群
血族婚	−/+	−	−
家族歴	−/+	−/+	−/+
凍瘡様紅斑の発症年齢	2m–5y	−	−/1m?
体幹の結節性紅斑	+/卄	+	+
周期熱の発症年齢	−/3m–8y	−	1m–1y
長く節くれだった指	+	+	+
関節拘縮	−/卄	卅	−
限局性脂肪萎縮	+/卄	卄	+
筋力低下	−/+	+	−
痙攣	−	+	−
多汗症	−/+	−	−
小球性貧血	−/+	卄	+
呼吸不全	−/+	−	−
心電図異常	np/LVH, LAD, CRBBB	?	np
肝脾腫	−/+	+	+
大脳基底核石灰化	−/+	+	−/+
PSMB8 遺伝子変異	p. G201V	p. T75M	p. T75M, p. C135X, 変異なし

（注：診断基準項目の背景を灰色で示した.）

で最も近いのはCAPS（クリオピリン関連周期熱症候群）と考えられるが，中條—西村症候群では関節炎を欠き，血清あるいは末梢血培養上清中のIL–1β過剰産生を認めない．一方．Weber-Christian病と診断されていたTRAPS（TNF受容体関連周期熱症候群）も報告されており，最終的には遺伝子診断が決め手になる場合もある[39]．

昨年，スペイン，アメリカ，フランスのグループとイスラエルのグループが，それぞれ姉妹例を含む4例と1例を新しい疾患Chronic atypical neutrophilic dermatosis with lipodystrophy and elevated temperature（CANDLE）症候群として報告した[26,27]．この疾患は中條—西村症候群の診断基準案8項目のうち家族内発症，皮疹，発熱，節くれだった指，脂肪萎縮，肝脾腫，大脳基底核石灰化の7項目を満たし，肉眼的にも酷似する．皮疹の病理組織像で好中球浸潤が目立ち，疾患名も好中球性皮膚症となっているが，主な浸潤細胞は異型を伴う大型の核をもつ組織球系細胞であり，中條—西村症候群の組織像と本質的には同様と思われる．さらにアメリカ，メキシコ，ポルトガルのグループは，兄妹例を含む3例をJoint contractures, muscular atrophy, microcytic anemia, and panniculitis-associated lipodystrophy（JMP）症候群（MIM#613732）として報告した[28]．この報告では鑑別対象として中條—西村症候群が挙げられ，よく似ているものの痙攣，貧血，知能低下の有無と脂肪萎縮の程度の違いから，同じ疾患である可能性は残るものの，異なるクラスターにまとめられた．肉眼的には，下半身に至る全身性の脂肪萎縮と手関節の強い屈曲拘縮を認め，中條—西村症候群よりも重篤な印象を与える．発熱はないが家族内発症，皮疹，（拘縮が強い）節くれだった指，（全身性）脂肪萎縮，肝脾腫，大脳基底核石灰化の6項目を満たす．昨年末，*PSMB8*遺伝子の中條—西村症候群とは異なるT75M変異が同定され，この変異によるキモトリプシン様活性の低下が確認されたことから，本疾患もプロテアソーム不全症であることが明らかとなった[29]．さらに最近，CANDLE症候群のスペイン系の症例にJMP症候群と同じT75M変異，ユダヤ系の1症例においてC135X変異が報告された[40]．これら3疾患の比較を表3にまとめた．

VII. 治療と経過，予後

ステロイド全身投与により皮疹は消失するが，減量により容易に再燃し，また脂肪萎縮には無効であ